https://doi.org/10.5194/egusphere-2023-1671
Preprint. Discussion started: 9 August 2023

Networks of geometrically coherent faults accommodate Alpine tectonic inversion offshore SW Iberia

Tiago M. Alves[1]

[1]3D Seismic Lab – School of Earth and Environmental Sciences, Cardiff University – Main Building, Park Place, Cardiff, CF10 3AT, United Kingdom

Correspondence to: Tiago M. Alves (alvest@cardiff.ac.uk)

Abstract. The structural styles and magnitudes of Alpine tectonic inversion are reviewed for the Atlantic margin of SW Iberia, a region known for its historical earthquakes, tsunamis, and associated geohazards. Reprocessed, high-quality 2D seismic profiles provide new images of 26 faults, which were mapped to a depth exceeding 10 km for the first time in this work. The faults are mostly syn-rift structures accommodating vertical uplift and horizontal advection (shortening) during Alpine tectonics. At a regional scale, tectonic reactivation has been marked by: a) the exhumation of parts of the present-day continental shelf, b) local folding and thrusting of sediment at the foot of the continental slope, and c) oversteepening of syn- and post-rift strata near reactivated faults (e.g. 'passive uplift'). This work proves, for the first time, that geometric coherence dominated the growth and linkage of offshore faults in SW Iberia; thus, they are prone to reactivate as a kinematically coherent fault network. Importantly, they form 100-250 km long structures, the longest of which may generate earthquakes with a momentum magnitude (Mw) greater than 8.0. Tectonic inversion started in the Late Cretaceous and its magnitude is greater close to where magmatic intrusions are identified at depth. In contrast to previous models, this work postulates that regions where Late Mesozoic magmatism was more intense comprise thickened, harder crust, forming lateral buttresses to NW-SE compression. It shows these structural buttresses to have promoted the development of early stage fold-and-thrust belts - typical of convergent margins - in two sectors of SW Iberia.

1 Introduction

Continental margins record complex post-rift tectonic histories, as fault reactivation and associated uplift are often controlled by structures inherited from their syn-rift evolution stages (Vasconcelos et al., 2019; Schiffer et al., 2020; Rodriguez-Salgado et al., 2023). Such a complexity is amplified when syn- and post-rift magmatism combines with far-field tectonics to affect distal offshore regions (Sun et al., 2020; Jolivet et al., 2021). For instance, local uplift and exhumation of older rocks on the Brazilian and West African margins were driven by important magmatism near the Walvis Ridge, Victoria-Trindade Seamount Chain, Pernambuco Plateau, Fernando de Noronha Seamounts, as key examples, in episodes that spanned several million years (Comin-Chiaramonti et al., 2011; Strganac et al., 2014; Teboul et al., 2017). In the South China Sea, evidence exists of important syn-breakup volcanism, which was complemented by post-rift magmatism near basin-bounding faults (Lei et al., 2020). Again, these phenomena occurred through a time-span of c. 32 Myr (Zhao et al., 2016; Sun et al., 2022). All these new

https://doi.org/10.5194/egusphere-2023-1671
Preprint. Discussion started: 9 August 2023

data stress a paradox in the published literature: while previous work tends to link regional magmatic processes to well-dated tectonic episodes, there is now increasing evidence that long-lasting post-rift tectonism is a key factor controlling the evolution of continental margins (Duarte et al., 2013; Casson et al., 2021).

In West Iberia, outcropping igneous rocks and offshore magmatic edifices have been correlated with distinct episodes of magmatism (Miranda et al., 2009; Pereira et al., 2022; Neres et al., 2023). Following the full separation of Iberia as an isolated tectonic plate, its Alpine-related evolution recorded counterclockwise rotation and subsequent collision with Eurasia (Pyrenean phase) and North Africa (Betic phase) (Vissers et al., 2016; Jolivet et al., 2021). Alkaline magmatism marked the first stages of collision between Iberia and Eurasia, near the Pyrenees, and has been associated with strike-slip tectonics and hotspot magmatism offshore West Iberia (Geldmacher et al., 2006; Miranda et al., 2009; Martín-Chivelet et al., 2019). Yet, an aspect not fully addressed in the literature concerns how this post-rift magmatism relates to the modern structural framework of its continental margin (Pereira et al., 2022). A deeper knowledge of the links between this post-rift magmatism and the structural framework of Iberia’s Atlantic Margin is crucial to understand its full tectonic and thermal evolutions. This is particularly the case for the more tectonically active, seismogenic region of SW Iberia (Fig. 1).

A second aspect not fully addressed concerns the stratigraphic record of Alpine tectonics in SW Iberia, as it is dominated by its younger Miocene pulse (Betic phase). Older Paleogene strata sampled onshore and in exploration wells are relatively thin, being also too sparse to provide a complete record of tectonic movement. Against this background, Maldonado et al. (1999) and Alves et al. (2003) used seismic and stratigraphic information to recognise Cenozoic phases of extensional collapse in west and south Iberia, an interpretation that contrasts with most offshore seismic data. In fact, widespread evidence for tectonic compression and widespread reactivation of syn-rift structures is observed offshore Portugal (Gracia et al., 2003; Terrinha et al., 2003; Neves et al., 2009; Duarte, 2013). In the particular case of the Atlantic margin of SW Iberia, Terrinha et al. (2003) suggested the presence of linked fault strands, none of which was capable of generating the Mw 9.0 Lisbon earthquake of 1755, but still long enough to consider them as loci for relatively large, proximal earthquakes. Terrinha et al. (2003) also suggested the presence of a ramp-flat structure at a depth of 6-8 km below the seafloor, with this structure being extensive enough to justify the combined reactivation of two of the largest faults on SW Iberia’s continental slope (TTR-10 and PSF). However, the interpretations in Terrinha et al. (2003) and more recent work were not accompanied by a detailed mapping of all major faults crossing SW Iberia using a comprehensive seismic-reflection dataset.

Key to proving a structural link between active, seismogenic faults is the recognition of their geometric and kinematic coherence (Walsh and Watterson, 1991; Walsh et al., 2003; Kim and Sanderson, 2005; Fossen and Rotevatn, 2016). Geometric coherence has been defined as the development of regular and systematic displacement patterns in a family of faults (Walsh and Watterson, 1991). In parallel, kinematic coherence reflects the existence of synchronous slip rates and slip distributions that are arranged such that geometric coherence is maintained (Peacock et al., 2002). These two types of coherence can occur for any fault types in nature; normal, strike-slip of reverse (Willemse et al., 1997; Davis et al., 2005; Song et al., 2020). While kinematic coherence is better established by documenting surface deformation after large earthquakes (Sachpazi et al., 2003; Elias and Briole, 2018; Karabulut et al., 2023), geometric coherence in seismic and outcrop data suggests strain in particular

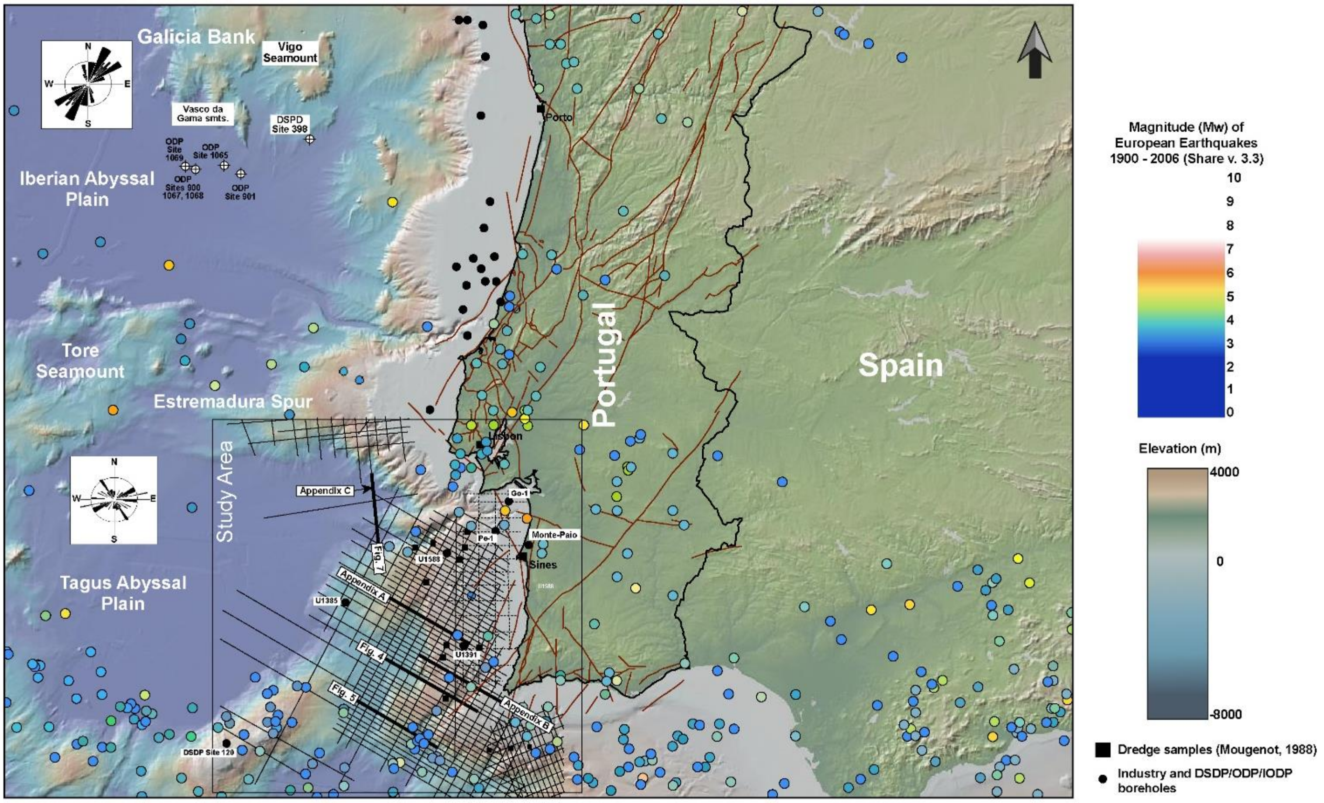

Figure 1: a) Bathymetric and topographic map from West Iberia highlighting the seismic and borehole datasets interpreted in this work, as well as main physiographic features and faults. The study area is shown within a black box together with the data set interpreted in this work. Also shown on the map are the locations and relative magnitudes of earthquakes for the period spanning 1900 to 2006, as obtained from GeoMapApp. The location and extent of onshore faults are taken from Cunha et al. (2019).

structures to be accommodated - at the geological time scale - as a continuum (Walsh et al., 2003). In other words, coherent sets of faults are able to accommodate strain by interacting in time and space, merging at depth to form continuous fault zones, i.e. fault displacement (and growth) are accommodated at the surface by discrete faults, but these same structures are linked as a continuous fault at depth (Giba et al., 2012). Importantly, geometric and kinematic coherence occur along a series of interacting fault strands when one considers the lateral growth of a fault zone, as in the example in Giba et al. (2012), but can also span a vast area, and multiple strands, when successive faults are kinematically related and linked. The best example of this areal span in geometric coherence is recorded by fold-and-thrust belts of accretionary prisms, which form complex fault networks posed to be reactivated in tandem during major seismogenic events, linked at depth by a common basal plate boundary thrust (Tsuji et al., 2014; Kimura et al, 2018).

https://doi.org/10.5194/egusphere-2023-1671
Preprint. Discussion started: 9 August 2023

This work goes beyond the published data to reveal that geometric coherence typifies the structural style of reactivated faults in SW Iberia. These faults have responded to NW-SE compression during the Late Cenozoic, a tectonic setting still active at present. As a result, tectonic uplift and horizontal advection (shortening) are accommodated by sets of faults revealing a coherent growth mode. Uplift and horizontal advection are also shown to be concentrated oceanwards from Late Mesozoic magmatic complexes. This interpretation has important implications for future geohazard assessments in SW Iberia, and to estimates of its seismogenic and tsunamigenic potential. In summary, this paper addresses the following research questions:

a) How can one quantify the magnitude of tectonic uplift and exhumation in proximal parts of reactivated continental margins using seismic reflection data?
b) In what ways tectonic uplift and exhumation relate to early magmatism along, and across, continental margins?
c) Which faults in SW Iberia record the greatest magnitudes of tectonic uplift and horizontal advection, and how they interact in time and space?

2 Geological Setting

2.1 Basement tectono-magmatic evolution

Basement units on the continental margin of West Iberia comprise a set of Variscan terrains whose limits and nature are yet not fully understood (Capdevilla and Boillot, 1988). Tectonic and geophysical data suggest the deep-offshore basins to be underlain by a tectonic terrain not identified onshore (Ribeiro et al., 2013), while other authors suggest these onshore Variscan terrains to extend oceanwards, under offshore sedimentary basins, complying with the general NW to ESE strikes of main faults and depocentres recognised in, and around, the Lusitanian Basin (Capdevilla and Mougenot, 1988). Recent Apatite fission-track analyses have shown sediment in the Lusitanian Basin to comprise a mix of lithological fragments of late Cryogenian to Ediacaran ages (Pan-African and/or Cadomian with peaks at 608-554 Ma) and Carboniferous to Permian ages (Variscan and post-Variscan, with peaks at 315-292 Ma) (Dinis et al., 2021). Some of these fragments are derived from both easterly and westerly sediment sources, show evidence of having been recycled from eroded sediment. They reflect the presence of basement lithologies that are different from the Variscan units now outcropping in Portugal and Spain (Dinis et al., 2021).

2.2 Syn-rift evolution of West Iberia

The West Iberian margin recorded continental rifting from, at least, Late Triassic to the Early Cretaceous, preceding a continental breakup phase that spans the latest Jurassic (Tithonian) to the Albian/Cenomanian (Alves and Cunha, 2018). Continental rifting was first widespread on the margin, with progressive lithospheric stretching and thinning resulting in a continental breakup event that propagated from SW to N Iberia, towards what is now the Bay of Biscay (Grevemeyer et al., 2022). In the specific case of SW Iberia, magmatism accompanied syn-rift tectonics in two main episodes: a) one at c. 200 Ma (Hettangian) associated with Central Atlantic Magmatic Province (CAMP) and essentially tholeiitic in nature, and b) a second episode dated from 135 Ma to 130 Ma (Valanginian) with a transitional affinity (Martins et al., 2008).

Continental breakup first started in what is now the Seine and Tagus Abyssal Plains by the latest Jurassic-earliest Berriasian and propagated along West Iberia, in a northerly direction, throughout the Early Cretaceous (Tucholke et al., 2007; Alves et al., 2009; Neres et al., 2023). Doubts still exist on the absolute timings of full, established breakup between West Iberia and Canada, though two important details have now been corroborated in the published literature: a) the J-anomaly is diachronous and reflects important magmatism associated with the northward propagation of continental breakup (Grevemeyer et al., 2022), b) the regional stratigraphy records two distinct tectonic pulses of continental breakup – one Berriasian-Aptian(?) associated with breakup offshore SW and Central Portugal, and a Late Aptian-Cenomanian associated with fully-established breakup in NW Iberia (Alves and Cunha, 2018). Recent data from Grevemeyer et al. (2022) and Saspiturry et al. (2021) indicate that the Late Aptian-Cenomanian stage marks the onset of lithospheric breakup west of Galicia into the Bay of Biscay.

At present, the continental slope of SW Iberia dips gently to the west due to the accumulation of thick Cretaceous-Cenozoic strata (Alves et al., 2009). However, important Late Cretaceous-Cenozoic exhumation and erosion are recorded on its proximal part, where the effect of Alpine tectonics and tectonic convergence with Africa were, and are still, significantly felt (Terrinha et al., 2003; Pereira et al., 2013). Furthermore, a major bathymetric feature separates SW Iberia from its NW part – the so-called Estremadura Spur – and was the locus of important post-rift tectonics and magmatism (Miranda et al., 2009) (Fig. 1). The evolution of the Estremadura Spur is associated with significant compressional tectonics and tectonic inversion in a style akin to a regional scale 'pop-up' structure (Ribeiro et al., 1990). This large pop-up structure trends roughly east-west and links onshore with the NE-SW-striking Central Iberian Range (Cunha, 2019).

2.3 Post-rift evolution

Post-rift tectonic reactivation started with the counterclockwise rotation of the Iberian Plate, formed after breakup in the Bay of Biscay and Pyrenees, and subsequent reactivation of older syn-rift structures (Saspiturry et al., 2020). After 80 Ma (Campanian), important magmatism occurred throughout Iberia (Martin-Chivelet et al., 2019). In SW Iberia, onshore and offshore alkaline magmatism is marked by the presence of sub-volcanic complexes near Sintra, Sines and Monchique (Figs. 1 and 2). Volcanic complexes also occur near Lisbon and offshore Algarve (Terrinha et al., 2009). Onshore, this Lower Cretaceous magmatism has been considered as ranging from ~94 Ma to 69 Ma (Miranda et al., 2009, Grange et al, 2010). Also recorded in this interval was the cessation of the former volcanism in the Basque Basin (Castañares and Robles 2004), while the Catalan Coastal Ranges recorded the intrusion of isolated, alkaline lamprophyres (Martin-Chivelet et al., 2019). The age of this magmatism is well constrained to ~79 Ma and is considered as marking the onset of Alpine shortening in the easternmost Pyrenean sector (Ubide et al., 2014).

Stratigraphically, Cenozoic tectonic reactivation and uplift are only partly expressed onshore, though important information can be gathered from the Lower Tagus and Alvalade Basins (Fig. 2). Reis et al. (2001) and Cunha (2019) correlate the Benfica Formation to the end of Pyrenean orogenesis and suggested an upper Eocene-Oligocene age for the continental strata forming this unit (Fig. 2). The thin Paleogene strata outcropping near Lisbon are overlain by a significant thickness of Miocene siliciclastics, which are associated in the literature with the Betic Orogeny of South Iberia (Fig. 2). Collision of the African plate with Iberia resulted in the subduction of oceanic crust near Gibraltar, and the orogenic episode that generated the Rif and Betic mountain ranges (Zitellini et al., 2009; Gutscher et al., 2012; Monna et al., 2015).

Onshore, stratigraphic information points out to a principal middle to late Miocene (Burdigalian to Tortonian) episode of deformation near Lisbon (Arrábida Range), while the Algarve Basin to the south records several stages of Miocene compression (Mougenot, 1988; Cunha et al., 2019). Generalised uplift of West Iberia's coastline is also recognised in the Pliocene-Quaternary and, locally, during major seismo-tectonic events such as the 1755 Lisbon Earthquake, which uplifted the Atlantic coast of Iberia in several locations (Silva et al., 2023). Neotectonic activity is also clear near reactivated structures such as the Pereira de Sousa Fault, the São Vicente Fault and multiple areas offshore Algarve (Terrinha et al., 2009; Somoza et al., 2021).

3 Data and Methods

3.1 Seismic-well correlations

This work uses regional (2-D) seismic data tied to exploration wells from SW Iberia, as shown in Fig. 1. The interpretation criteria of Alves et al. (2009) and Pereira et al. (2013) are used to map and recognise main seismic-stratigraphic units, reactivated syn-rift structures and associated magmatic edifices. Unpublished information from exploration wells Pe-1, Go-1 and Monte Paio-1, together with dredge data published in Mougenot et al. (1979) and Mougenot (1988), are used to date main seismic-stratigraphic markers and strata (Fig. 1). These data are complemented with information from DSDP Site 120 and IODP Sites U1385, U1391 and U1588 which recently drilled the SW Iberian margin (Hernández-Molina et al., 2013; Hodell et al., 2023) (Fig. 1). All data were fully integrated in a Schlumberger's Petrel® project so that structural, magnetic and seismic stratigraphic data can be analysed together.

Main seismic-stratigraphic markers are interpreted across the study area and, whenever possible, corroborated with information from DSDP and IODP Sites U1385, U1391 and U1588 (Fig. 2).

https://doi.org/10.5194/egusphere-2023-1671
Preprint. Discussion started: 9 August 2023

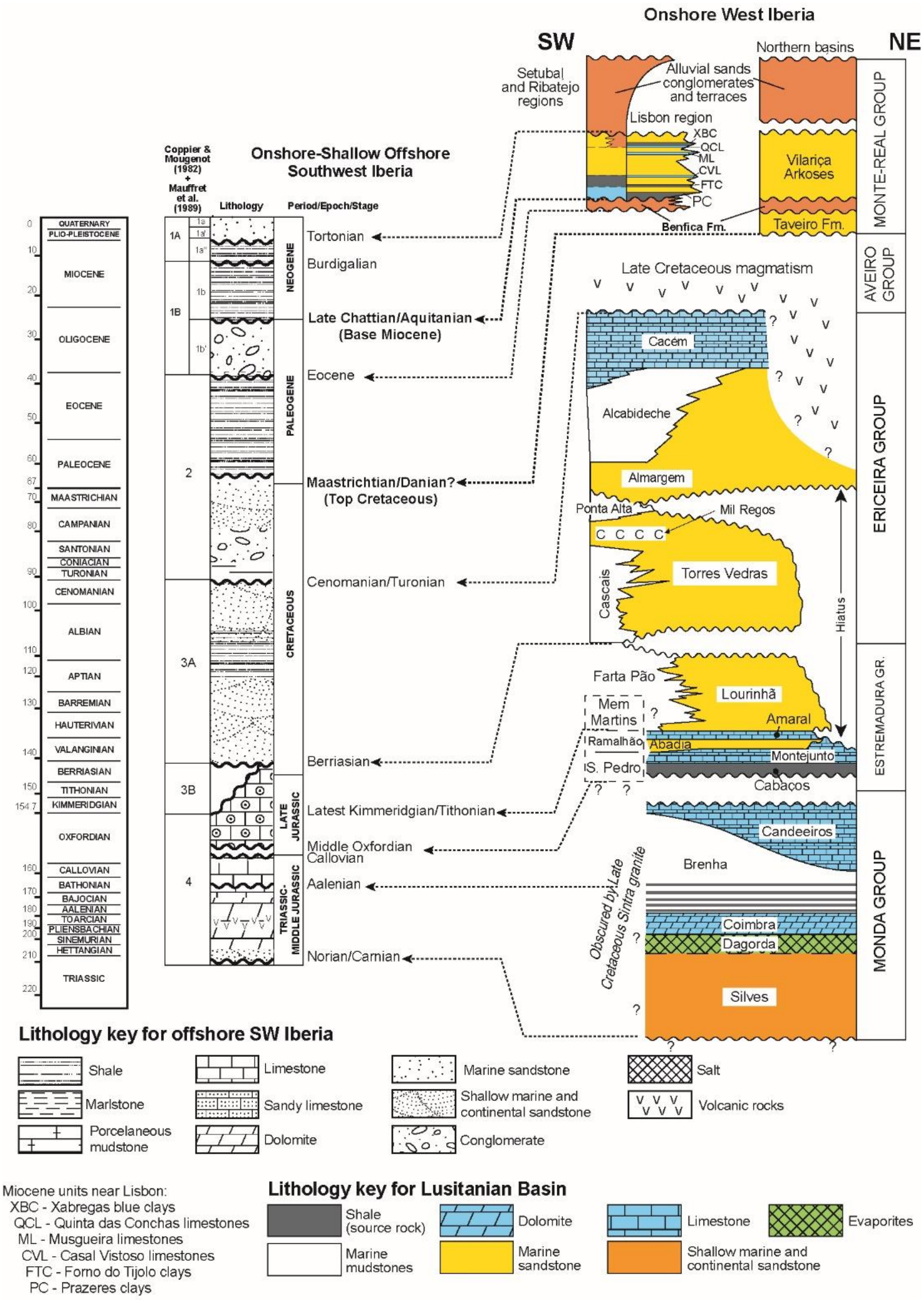

Figure 2: Stratigraphic panel correlating the main seismic-stratigraphic units offshore SW Iberia with the known stratigraphy of the Lusitanian, Lower Tagus and Alvalade Basins (onshore West Iberia). Major seismic-stratigraphic markers in our interpretation include the base of the Miocene sequence and the Top Cretaceous unconformity, as highlighted on the panel.

3.2 Kinematic data revealing tectonic uplift and horizontal advection

An important aspect of this study concerns the mapping and quantification of tectonic uplift, horizontal advection, and folding. In this work, the quantification of tectonic uplift and horizontal advection is based on the criteria illustrated in Fig. 3 (He et al.), together with the recognition of major depositional hiatuses along areas that were uplifted on the SW Iberia, i.e. the erosion or not deposition of Late Mesozoic-Cenozoic megasequences that are, on the continental slope and rise, well developed and oversteepened.

The kinematic models in Willet et al. (2001), Willett and Brandon (2002) and, more recently, He et al. (2021) recognise a significant difference between convergent and extensional regions in terms of their inherent deformation styles (Fig. 3). Contraction of the upper crust will cause the strata subjected to such process to fold or oversteepen, maintaining the bed-parallel geometries of strata that precede such a contraction (Fig. 3). In other words, tectonic contraction will oversteepen the hanging-wall strata of a thrust (or fold) in its direction of vergence without imposing any thickness variations (growth or erosion) to older strata deformed below the seafloor (Fig. 3). Key stratigraphic markers that precede the deformation phase will be tilted and deformed, but without revealing strata growth near the fault. In contrast, regions experiencing extension will deform to accommodate vertical subsidence on their hanging-wall blocks, and uplift on footwall blocks, with the difference in level between the two leading to important growth of strata in syn-tectonic hanging-wall basins (Fig. 3). It is thus important to stress that the growth of strata accompanies subsidence in extensional settings, while folding and thrusting is expected in areas experiencing contraction, accompanying tectonic uplift. If one has reliable stratigraphic markers - originally laid in an horizontal position on a continental margin - that were repeatedly oversteepened on a continental slope, a minimum value for uplift and exhumation can be estimated taking into account the palaeotopography of a continental margin.

In summary, by mapping throws, dips and level differences in key seismic-stratigraphic markers, one can estimate the minimum tectonic uplift and horizontal advection recorded by particular structures after their syn-rift (extensional) stage. This method is akin to the collection of the throw-depth (T-Z) and throw-distance (T-D) data necessary to characterise the modes of fault growth in normal fault arrays (Walsh and Watterson, 1991; Walsh et al., 2003). The two key seismic-stratigraphic markers considered in this study consist of the Top Cretaceous and Base Miocene unconformities, as also identified in Gracia et al. (2003), Terrinha et al. (2003), Alves et al. (2009) and Terrinha et al. (2009).

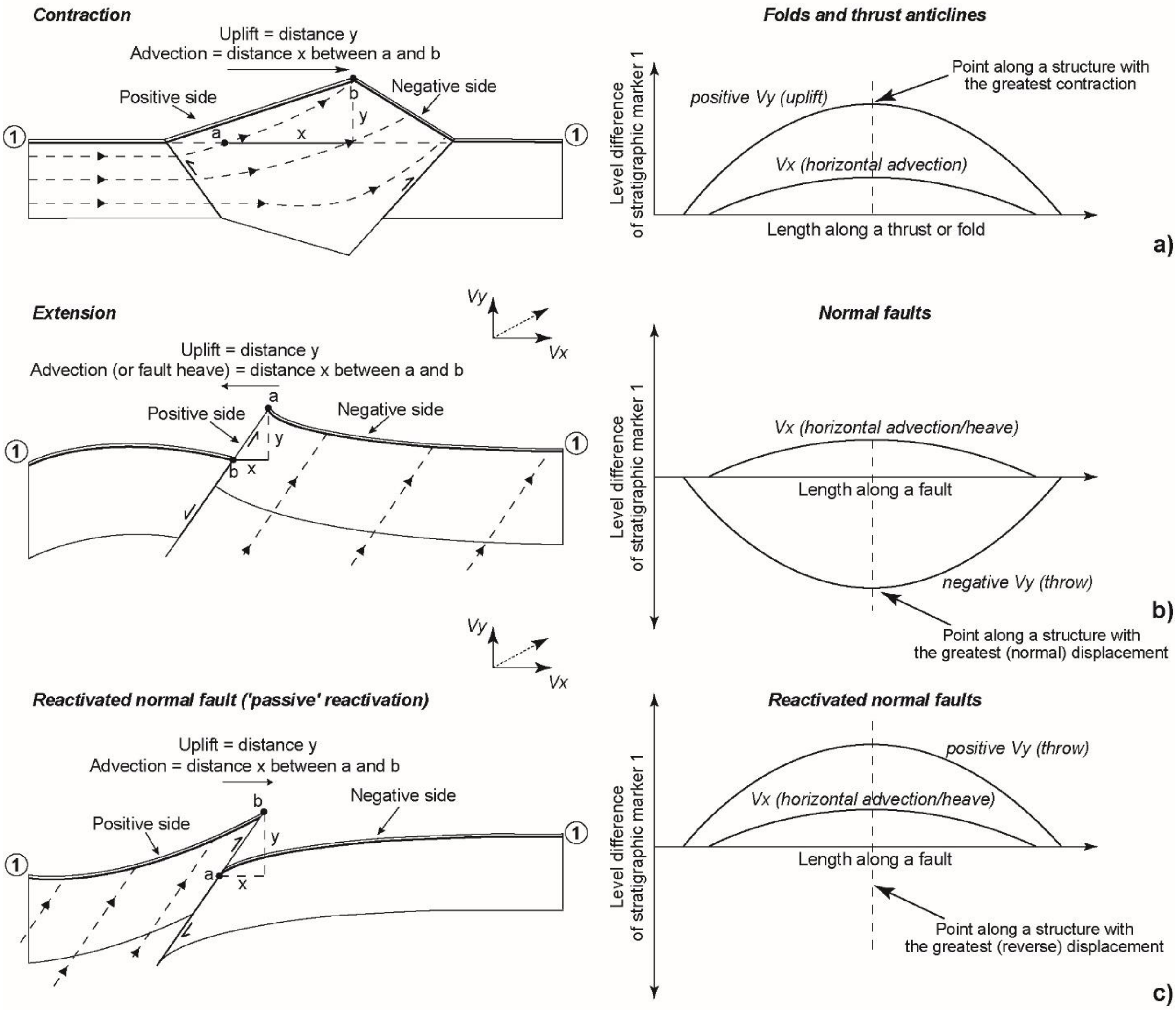

Figure 3: Kinematic models for tectonic uplift and horizontal advection as modified from He et al. (2021). Material transport in each of these structures is marked as dashed lines with arrows. Material transport in these three cases has vertical (Vx) and horizontal components (Vy). In all configurations, advection is from the positive side to the negative side. a) uplift and 210 horizontal advection in folds and thrust anticlines, with level difference of stratigraphic marker indicating a positive variation for both parameters. b) uplift and horizontal advection in and extensional setting, with horizontal advection resulting in a positive value but uplift being negative (subsidence). c) uplift and horizontal advection for the case of a normal fault reactivated under a compressive setting, with both uplift and horizontal advection being positive in value. In the normal fault case above an uplift of zero (0) is assumed in this work for the sake of simplicity.

4 Reactivated offshore structures

Figures 4, 5 and 6 show the main structures mapped offshore SW Iberia. A series of NNE-SSW to NW-SE normal faults compose the structural framework of the margin, and often interact spatially to form a mosaic of sub-basins and minor depocentres. High-amplitude folds and pervasive faulting of Mesozoic and early Cenozoic strata are observed in seismic data. Well-developed, reactivated tilt blocks are recognised to the west, oceanwards of Fault 3 – the Slope Fault System (SFS) of Alves et al. (2009) and the Pereira de Souza Fault (PSF) of Terrinha et al. (2003) (Figs. 4 and 5). Importantly, the region east (landwards) of Fault 3 reveals relatively thin, and exhumed, Mesozoic rocks (Fig. 4).

This character accompanied the oversteepening of post-rift strata on the continental slope, where erosion and exhumation of basement rocks are also observed east of Fault 3 (Figs. 4, A1 and A2).

5 Kinematic indicators of tectonic uplift

5.1 Syn-rift structures reactivated as reverse faults, thrusts and thrust anticlines

The clearest example of tectonic reactivation in SW Iberia concerns the inversion of syn-rift normal faults, which were mostly west-dipping during the Mesozoic as east-dipping thrust faults. Figures 4 and 5 show examples of such reactivation in SW Iberia, downslope from the shelf-edge and near Fault 7 (the Marquês de Pombal Fault cf. Terrinha et al., 2003) (Fig. B). Slope strata are deformed, oversteepened and locally thrusted, contrasting with the style observed west of Fault 3 (Pereira de Sousa Fault; Terrinha et al., 2003). In the particular case of Fault 7, the seismic data show evidence for the rooting of thrusts and reverse faults on syn-rift horsts, which are offset at depth (Fig. 5).

Further north, the past imposition of a rough N-S direction of compression in the Estremadura Spur has reactivated previous syn-rift faults as steep thrust faults and related anticlines, particularly near the edges of the Spur as a bathymetric feature (Figs. 6 and 7). Other anticlines and local pop-up structures occur throughout the Estremadura Spur, some of which are related to the presence of buried igneous intrusions at depth.

5.2 Asymmetrically uplifted (and exhumed) strata on the footwall of thrust faults

Deformed and oversteepened strata on the footwall of thrust faults are another diagnostic feature of tectonic uplift and compression (Figs. 4 and A2). Such strata were, during syn-rift extension, east-dipping, or formed relatively flat depocentres formed in sediment-filled conditions, revealing stratal growth onto faults located to their east. They are now oversteepened and tilted to the west (Fig. 4 and A2). Many of these oversteepened, uplifted strata not only terminate against Fault 3, which has previously been interpreted as part of a major slope bordering fault system (SFS, Alves et al., 2009), but also onto other reactivated faults and horsts on the continental slope.

The fact that strata in these conditions can be correlated across faults, not constituting offlapping sediment which bypassed the slope topography, make them useful in the quantification of cumulative tectonic uplift on the margin, an aspect addressed in Section 6 in this paper.

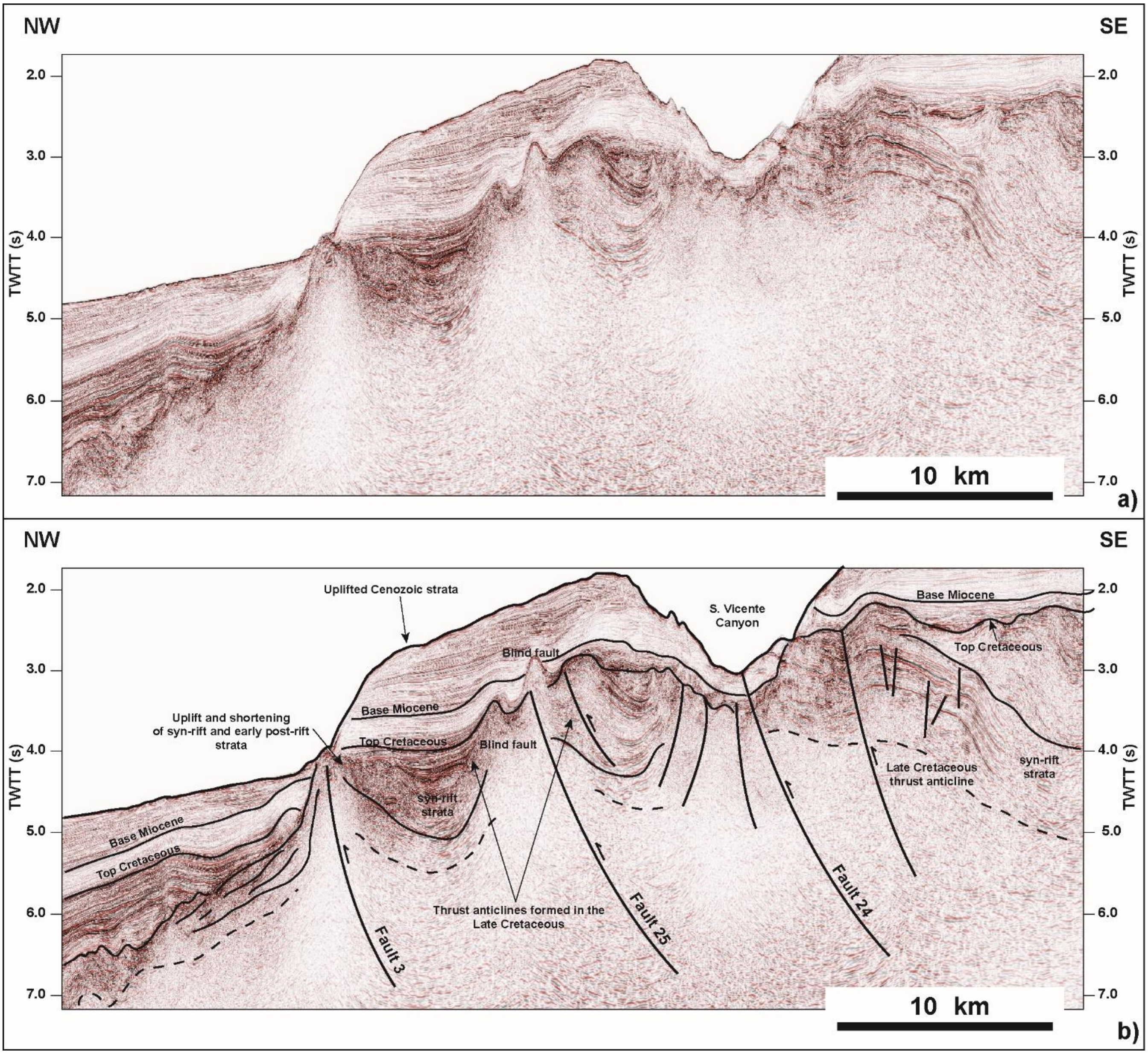

Figure 4: a) Uninterpreted and b) interpreted seismic profile from SW Iberia highlighting the presence of a series of syn-rift faults reactivated as large reverse faults and thrusts. Key seismic stratigraphic markers and units are also indicated in the figure, as well as the location of the S. Vicente Canyon. Note the degree of tectonic uplift recorded to the SE of Fault 3 and the marked Late Cretaceous erosion and folding imaged on seismic below the Top Cretaceous unconformity. The location of the seismic profile is shown in Fig. 1. Seismic data courtesy of TGS.

https://doi.org/10.5194/egusphere-2023-1671
Preprint. Discussion started: 9 August 2023

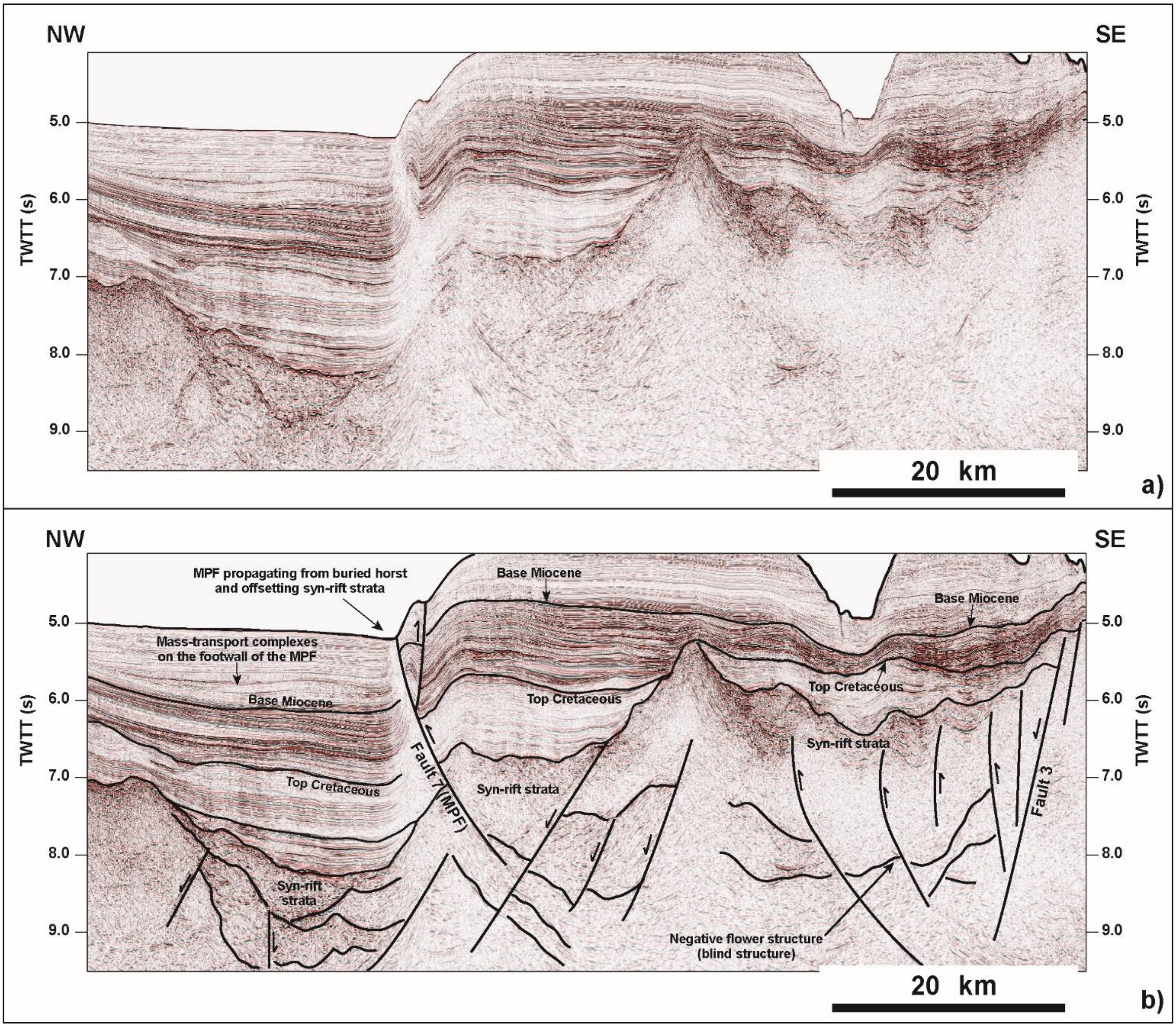

Figure 5: a) Uninterpreted and b) interpreted seismic profile across the Marquês de Pombal Fault (Fault 7) revealing this fault as offsetting syn-rift strata and rooting at a depth of c' 9.0 twt. Of importance is also the presence of a negative flower structure in what is the southern tip of Fault 3. The location of the seismic profile is shown in Fig. 1. Seismic data courtesy of TGS.

5.3 Vertically uplifted slope terraces and associated syn-rift topography

On proximal parts of the West Iberian margin, correlative strata on the shelf and upper continental slope can be offset by several 100s of metres by thrust faults and inversion structures (Figs. 4 and 5). This is most relevant when key stratigraphic markers are mapped across these inversion structures such as: a) the Cenomanian limestones of the Cacém Formation, which reveal a relatively constant thickness of 120-150 m in the Lusitanian Basin and immediate continental slope (see Alves et al. 2003, Alves et al., 2009), b) Upper Cretaceous sills and magma flows associated with a buried magmatic complex, c) the Base Miocene unconformity recognised in seismic data by Mougenot et al. (1988) and by recent IODP Sites in SW Iberia (Fig. 1). At present, many of these structural terraces are also dipping oceanwards from faults, revealed a mixed style of tectonic deformation that is akin to that described in Section 5.2.

Figures 4 and 7 show examples of uplifted terraces from distinct parts of West Iberia. Figure 4 reveals uplift of the shelf edge as correlative strata on the continental slope dip to the west due to compression and uplift of the continental shelf of SW Iberia (Sector 3). In Figure A2 a similar geometry is observed in slope deposits of the Central Sector, which dip to the west and are deformed at depth. They occur together with the marked folding and truncation of Cenozoic and Upper Cretaceous strata just below the seafloor. Other examples of deformed, uplifted syn-rift topography are mapped in several parts of SW Iberia as highlighted in the following section.

6 Quantification of tectonic uplift and horizontal advection

The tectonic framework of the basement of SW Iberia is, at present, interrupted by magnetic anomalies as shown in Fig. 6. These anomalies correlate with the presence of Late Cretaceous magmatic intrusions in the Central and SW sectors of West Iberia (Terrinha et al., 2018; Neres et al., 2023) and older Variscan granites in NW Iberia. Following the methodology in this paper, Figure 8 shows a graphical representation of local uplift and horizontal advection associated with fault reactivation for the entire Atlantic margin of SW Iberia. The data plotted in Fig. 8 highlight important differences amongst the magnitude of uplift and horizontal advection recorded by the faults mapped in this work. By comparing the graphs in Fig. 9 with the latter maps it becomes clear that the principal structures accommodating tectonic inversion in SW Iberia are Faults 3, 7 and 11. Of particular interest is the recognition of a corridor of deformation near the Sines Magmatic Complex and its offshore continuation (Figs. 6 and 8). Over the areas where these anomalies occur, no major fault reactivation is recorded (e.g. Faults 12, 13, and 26). In contrast, all faults show enhanced uplift and horizontal advection west of Fault 12 and the offshore prolongation of the Sines Magmatic Complex (Fig. 8). This is interpreted as proving a clear effect of sub-surface magmatic bodies on the magnitude of tectonic reactivation in SW Iberia, particularly west of the Sines Magmatic Complex and between this latter and the Estremadura Spur further north (Figs. 5, 7 and 8). In this more central region of West Iberia, the broad intrusion of Late Cretaceous magma uplifted the so-called Estremadura Spur before the main phases of Cenozoic compression,

https://doi.org/10.5194/egusphere-2023-1671
Preprint. Discussion started: 9 August 2023

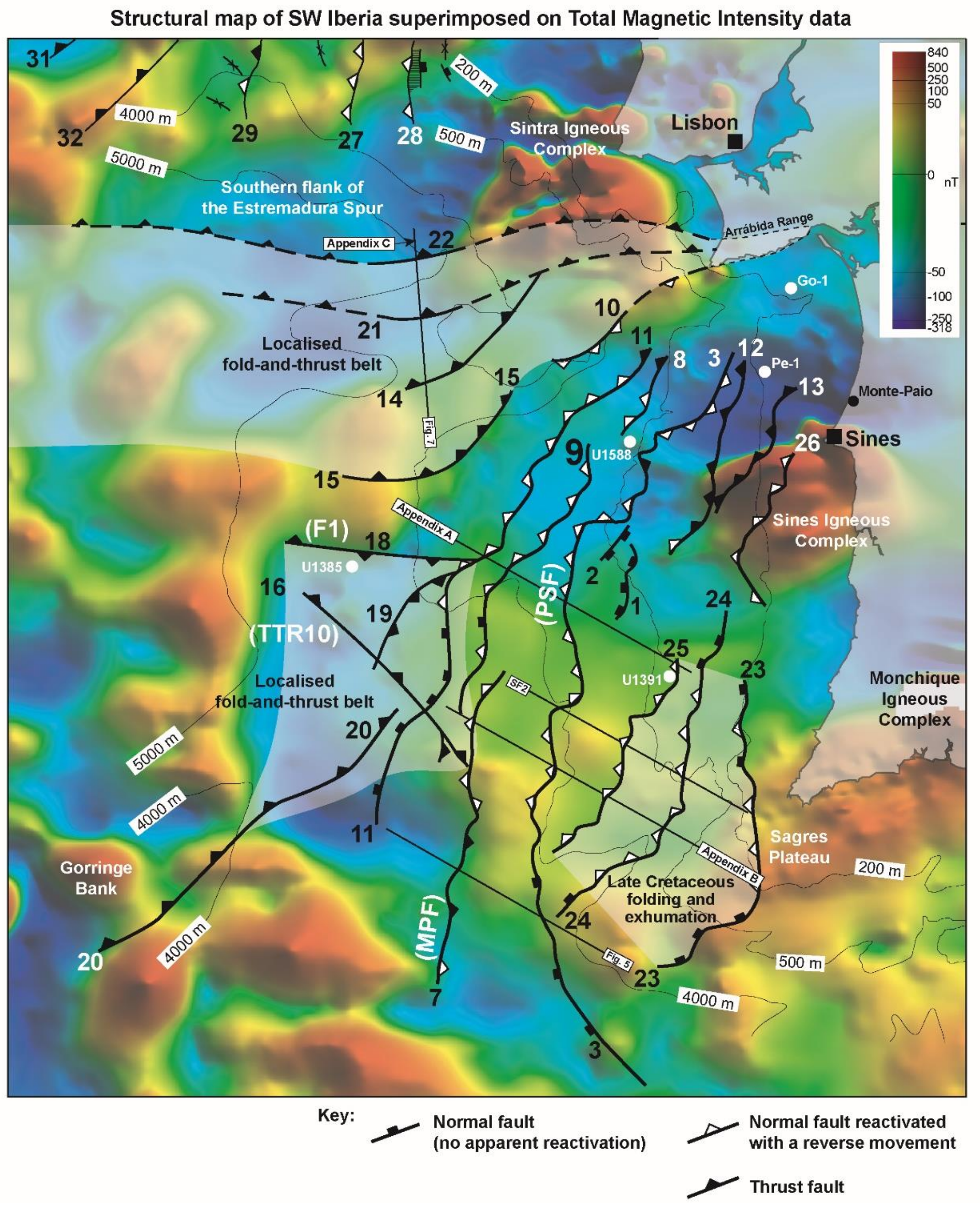

Figure 6: Structural map of SW Iberia superimposed on Total Magnetic Intensity data (TMI). The map reveals a presence of localised, early-stage fold-and-thrust belts between the Sintra and Sines Magmatic complexes, and west of this latter. Structures mapped constitute long fault zones that are hard linked at depth to constitute >200 km long features. TMI data provided by Getech UK.

https://doi.org/10.5194/egusphere-2023-1671
Preprint. Discussion started: 9 August 2023

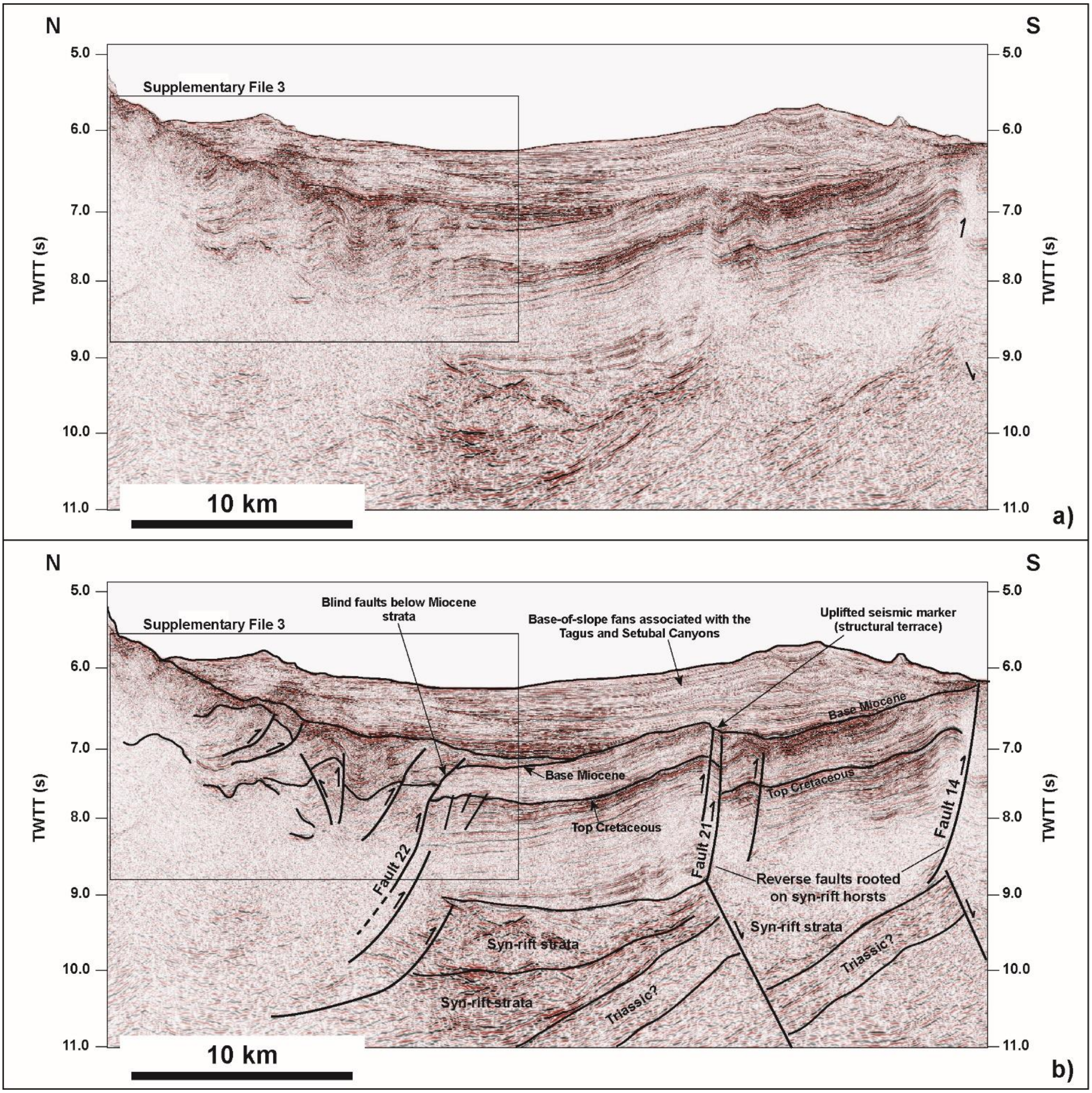

Figure 7: a) Uninterpreted and b) interpreted seismic profile from the southern flank of the Estremadura Spur highlighting the presence of a localised fold and thrust belt. Theis area of significant folding continues eastward towards the Arrábida Chain. Note the presence of bling faults below the Miocene-Holocene strata in the figure. The location of the seismic profile is shown in Fig. 1. Seismic data courtesy of TGS.

and made this sector structural higher (uplifted) in relation to the cooling, subsiding Tagus and Iberian Abyssal Plains that surround it.

Further south, the magnetic anomalies that extend offshore from Sines indicate the presence of a vast area intruded by Late Cretaceous magma (Figs. 6 and 8). When interpreting the graphs and maps in Figs. 8 and 9, it becomes clear that the area intruded by this Late Cretaceous magma records limited faulting and constitutes a structural buttress in front of which most of the uplift and horizontal advection is accommodated by Fault 3 and major thrusts oceanwards from this latter structure.

Another key aspect is that the structures mapped in this work consist of large fault corridors at depth, essentially syn-rift normal fault strands that were hard-linked during Alpine-related compression. In contrast to previous data in Terrinha et al. (2003), the faults which accommodated most of the Cenozoic compression are not frontal thrusts of a relatively shallow basal detachment. Instead, the set of faults occurring on the mid-continental slope – Faults 3, 7, and the northern part of Fault 11 – together record the greatest values of uplift and horizontal advection. Their lower tips are either rooted in (or offsetting) syn-rift strata or link to syn-rift faults deeper in the crust. In addition, Faults 23, 24 and 25 are also important structures accommodating strain to the northwest of the Monchique Magmatic Complex and the Sagres Plateau (Figs. 6 and 8).

7 Discussion

7.1 Structural controls on Alpine deformation offshore West Iberia

The data in this paper point out to important tectonic reactivation of SW Iberia since the Late Cretaceous, first associated with the intrusion of magma in parts of its proximal margin and on the Estremadura Spur, and later via the reactivation of syn-rift faults, which became laterally linked structures along the West Iberia margin (Fig. 8). Relatively large igneous edifices occur in Central and SW Iberia, namely the Fontanelas Volcano (Pereira et al., 2021), together with large buried magmatic bodies in SW Iberia (Fig. 6). The fact these sills are known to be Upper Cretaceous in age (Miranda et al., 2009; Pereira and Gamboa, 2023) makes them very good stratigraphic markers for uplift in the areas they are imaged.

This work interprets the effect of the largest of these igneous edifices to have been significant in the deformation history of SW Iberia. On the Estremadura Spur, a level difference of ~ 4000 m is observed at present between the upper continental slope and the Tagus Abyssal Plain. The recognised pop-up structure that forms the Estremadura Spur at present may have been first thermally uplifted and then folded, accommodating great part of this deformation on its southern and northern flanks (Fig. 7). It is also accommodated at the base of the slope, south of the Estremadura Spur, by an early-stage fold-and-thrust belt, as highlighted in Figs. A3 and A4. The impact of igneous intrusions in local strata deformation is also recorded at a local scale, with anticlinal structures and oversteepened, folded strata accompanying deep intrusions (Pereira and Gamboa, 2023).

A broader effect of magmatic intrusions on local uplift and deformation is observed in SW Iberia. East of Fault 3, towards Sines, occurs a plateau region with relatively little fault reactivation. Fault-related uplift and horizontal advection is much more

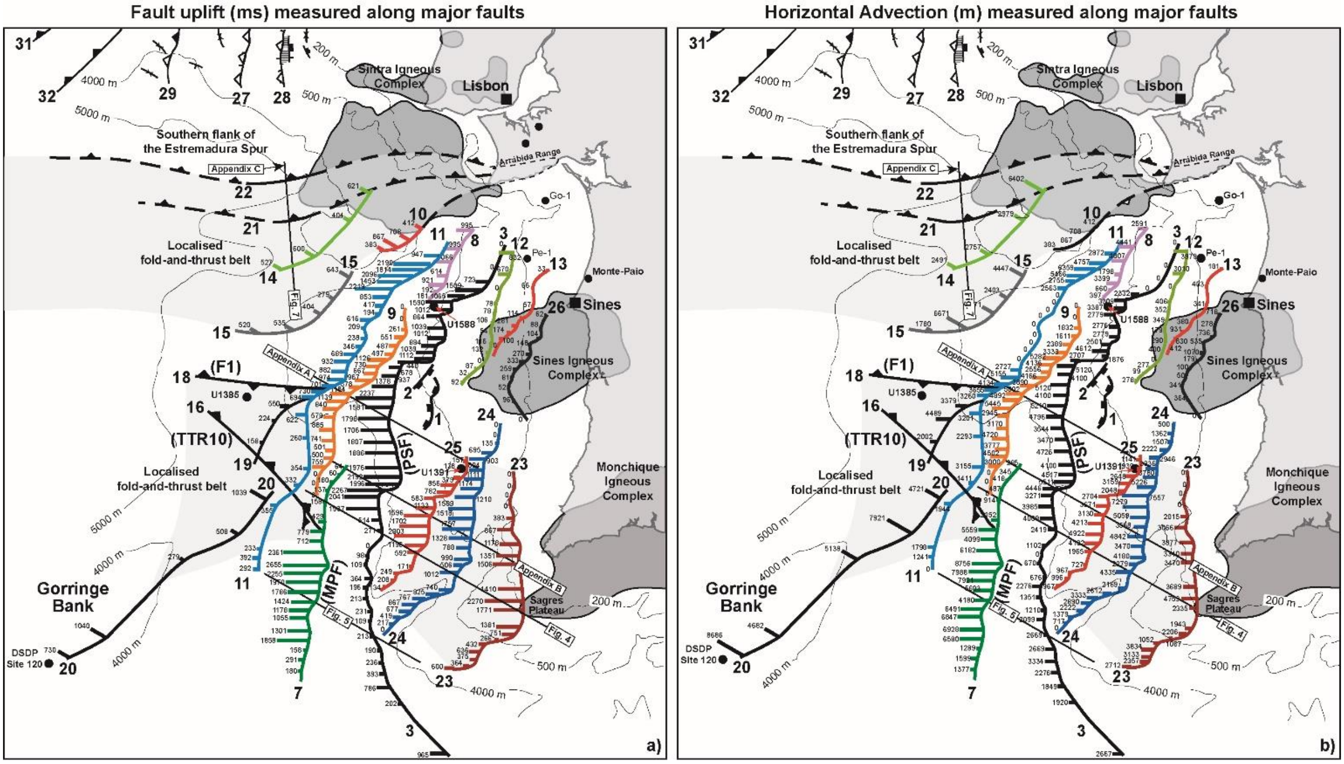

Figure 8: Graphical representation of fault uplift and horizontal advection as measured for each fault (see Supplement A and Figure 9 for detailed data). The data show Faults 3, 7 and 11 as being the structures accommodating most of Alpine compression in SW Iberia. Also important are Faults 24 and the joint Faults 14 and 15 to the northwest of the study area.

pronounced west of this plateau where Late Mesozoic igneous intrusions are recorded on seismic and magnetic data (Figs. 6 and 8). The effect of such promontory is discussed in more detail in the following section.

At a local scale, seismic lines through several reverse faults and thrusts demonstrate a close control of syn-rift structures on the growth and propagation of younger faults. In the particular case of Fig. 5, the Marquês the Pombal Fault is shown to be in part rooted on a syn-rift tilt block, with clear evidence for displacement of syn-rift units at the tip of this same tilt block. When this displacement is not clear in seismic data, strata near the Marquês de Pombal Fault reveal the propagation and development of splays of faults rooted on the tips of tilt blocks and other structural highs (Fig. 5).

A similar structural style is observed offshore Lisbon, on the southern foot of the Estremadura Spur. Here, the putative NW-SE oriented compression accommodated by base-of-slope strata is accommodated by a series of ENE-WSW thrust faults that root at the tips of syn-rift tilt blocks (Fig. 7). In addition, several sets of folds and thrusts are imaged in this same seismic profile in Fig. 7. Above the tilted syn-rift blocks, Mesozoic strata were deformed in a series of low-amplitude thrust anticlines and corresponding thrust faults, which are spaced at ~ 20 km replicating the spacing of syn-rift blocks below (Fig. 7). Such an architecture resembles one of an early-stage accretionary prism; in this case revealing a clear vergence of thrust anticlines to the south and recording a style of disharmonic folding that differs from younger strata. Above this first set of thrust anticlines occurs a more localised base-of-slope complex showing tight folding and deformation with a wavelength of ~ 4 km (Figs. 7 and A3). While the deeper, lower amplitude fold-and-thrust belt developed as an offshore continuation of the onshore Arrábida Range – a folded succession of syn-rift deposits that delimits structurally the region south of Lisbon – the shallower complex is akin to gravitational complexes associated to transpressional tectonics that are recorded in Equatorial Brazil and Southern Italia, to cite two key examples (Davison et al., 2016; Mangano et al., 2023). This work thus postulates that such a complex folding results from distinct tectonic pulses associated with the Alpine Orogeny. The older fold-and-thrust complex is capped by relatively underformed Upper Cenozoic strata, including the base-of-slope deposits that derive from the Cascais, Lisbon and Setubal Canyons, and shows Upper Cretaceous volcanicastic sediment from the Lisbon Volcanic Complex deformed below a Cenozoic unconformity (Fig. 7). Above the latter volcaniclastic deposits is imaged the smallest of fold-and-thrust complexes, above which the same upper Cenozoic sediments are also relatively undeformed (Fig. A3). It is therefore interpreted that the base of these underformed Cenozoic strata is Miocene in age (Mid Miocene?) and associated with the paroximal stage of Alpine tectonics in West Iberia (Cunha et al., 2019). The largest of thrust faults deformed latest Cretaceous and Paleogene strata and may have been first active during the Oligocene – either by early stage tectonic deformation associated with the Betic compression phase, or at the end of Pyrenean tectonics. These thrusts are seemingly active at present, and were likely first formed during the earliest episodes of Cenozoic compression, perhaps starting during the later stages of Pyrenean tectonics, with main thrust faults having been reactivated in successive stages since then. Therefore, many (if not the most) of the inversion structures imaged in seismic data in SW Iberia are likely to have been reactivated in multiple episodes, potentially also as blind faults at depth with no seafloor expression (Figs. 4, 5 and 7).

7.2 Significance of geometric coherence in adjacent reactivated faults

Geometric and kinematic coherence have been considered in the literature as proving the development of regular and systematic displacement patterns in related fault families (Walsh and Waterson, 1991; Walsh et al., 2003; Kim and Sanderson, 2005). Detailed measurements of uplift and horizontal advection for the faults mapped in SW Iberia reveal a clear geometric coherence (Figs. 9 and 10). Cumulative data for fault uplift and horizontal advection show typical coherent profiles in which the values recorded at the mid-part of SW Iberia, offshore Sines, are greater than on the its northern and southern limits (Fig. 10a,b). The faults bordering the Estremadura Spur were excluded from our analysis as they show bathymetric differences of more than 4000 metres, and part of this difference may be due to thermal cooling and subsidence of the Tagus Abyssal Plain. In SW Iberia, Faults 3 and 7 are seen as accommodating most of tectonic uplift, while Faults 7 and 24 record the greatest horizontal advection (Fig. 9). In the particular case of the N-S Fault 3, the Slope Fault System of Alves et al. (2009), Fig. 9 reveals it as a coherent structure along strike that is kinematically linked through a distance of ~ 200 km. Such a characteristic, together with the similar profiles for cumulative uplift and horizontal advection, are clear indicators of geometric and kinematic coherence. The cumulative data in Fig. 10a,b also show a typical C-shaped profile along SW Iberia, which is typical of coherent

https://doi.org/10.5194/egusphere-2023-1671
Preprint. Discussion started: 9 August 2023

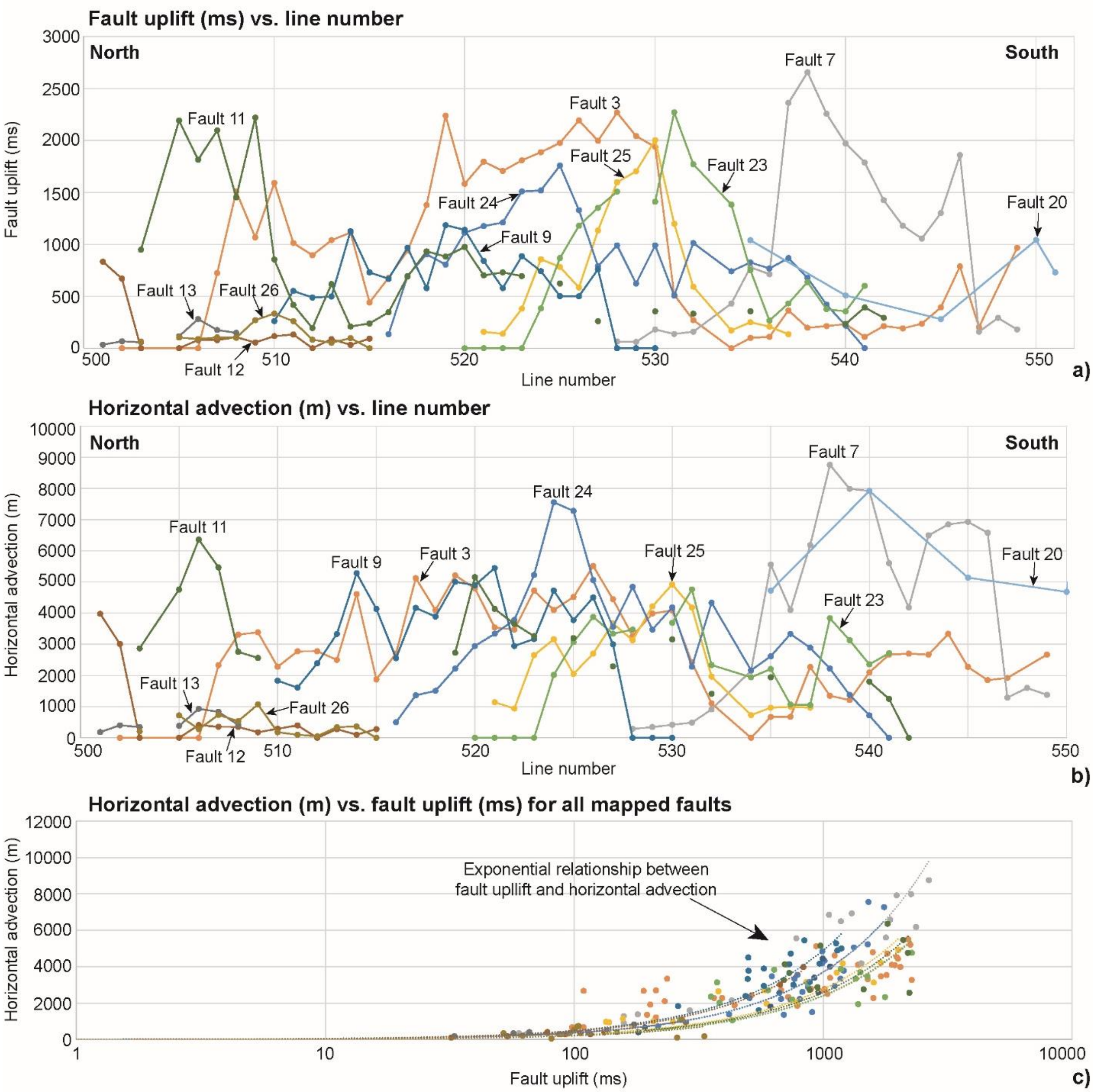

Figure 9: Graphs highlighting the distribution of fault uplift and horizontal advection in a north to south direction along SW Iberia. a) Relatively large values of uplift are recorded for Faults 3, 7 and 11. b) Horizontal advection is larger for Faults 7, 11 and 24, with Fault 20 also presenting a large value. C) Plot of horizontal advection (m) vs. fault uplift (ms) for all mapped faults. The graph highlights the exponential relationships between these two properties for all the structures mapped. 400

fault networks. This naturally means that not all the faults in this network will be reactivated in a single seismic event, but that the rate in which the all systems of faults grew is coherent and reflects the development of a linked fault network in SW Iberia. It also suggests that the sequential movement of this fault network is an important phenomenon in the study area, confirming the postulate of Walsh and Watterson (1991). They stated that forward, rearward and lateral propagations in fault arrays are equally important when fault coherence is confirmed, in away replicating the setting of convergent margins such as SE and E Japan (Tsuji et al., 2014; Kimura et al, 2018) and other areas recording significant tectonic shortening. However, the quantification of cumulative uplift and horizontal advection values in this work also indicates that the magnitudes of tectonic reactivation were greater near structural barriers (buttresses) between the Estremadura Spur and Sines, as northwest of the offshore prolongation of the Monchique Magmatic Complex. There is a difference in cumulative uplift and horizontal advection as one reaches these regions.

Comparing Figs. 6 and 8 with fault data provides a robust correlation amongst the areas affected by important tectonic compression and the Sines Magmatic Complex. Note that several igneous edifices occur west of the Sines Magmatic Complex in SW Iberia. These igneous edifices are also imaged in seismic data, coincide with local horsts, seamounts (e.g. Descobridores Seamounts) and are often bounded by thrust faults propagating from deeper parts of the crust to delimit a proximal sector of SW Iberia that was tectonically uplifted in the Late Cretaceous-Cenozoic.

7.3 Implications for future geohazard assessment

A first implication of this work is that a coherent fault mode hints at the possibility of reactivating SW Iberia through a broad area during large seismic events. In such a setting previous fault configurations, limited to proposing the lateral reactivation of two-three faults strands, is further complemented in this work by the possibility of reactivating faults that are sequentially placed forward or rearwards of the MPF and TTR10 faults mapped by Terrinha et al. (2003). Thus, the model in this work suggests that fault displacement can be kinematically accommodated by multiple strutures during a large seismic event, increasing the seismogenic and tsunamigenic potentials of SW Iberia. The recognition of a > 200 km long Fault 3, for instance, suggest the potential to generate Mw 8.0 earthquakes in this structure alone (Wyss, 1979; Bonilla et al., 1984; Trippeta et al., 2019).

The presence of structural buttresses rearwards from the continental slope, at the approximate latitude of Sines and near the Sagres Plateau, has also implications regarding the seismogenic potential of the margin. This work suggests that areas where Late Cretacous magmatism was more intense, and magma intruded the crust in greater volumes, are structurally harder, and more stable, than the regions not affected by this magmatism. They were also thermally and mechanically uplifted at the start of the Alpine tectonics, generating structural ‘indentors’ – namely parts of the continental margin that formed hard buttresses to tectonic shortening occurring in a N-S and NW-SE direction during the Cenozoic. This paper also stress the presence of immature fold-and-thrust belts south of the Estremadura Spur – itself interpreted as a large pop-up structure by Ribeiro et al. (1990) – and west of Sines (Figs. 6, 7 and 10c,d). On the same token, the presence of hard magmatic ‘core’ of rock at Sines

https://doi.org/10.5194/egusphere-2023-1671
Preprint. Discussion started: 9 August 2023

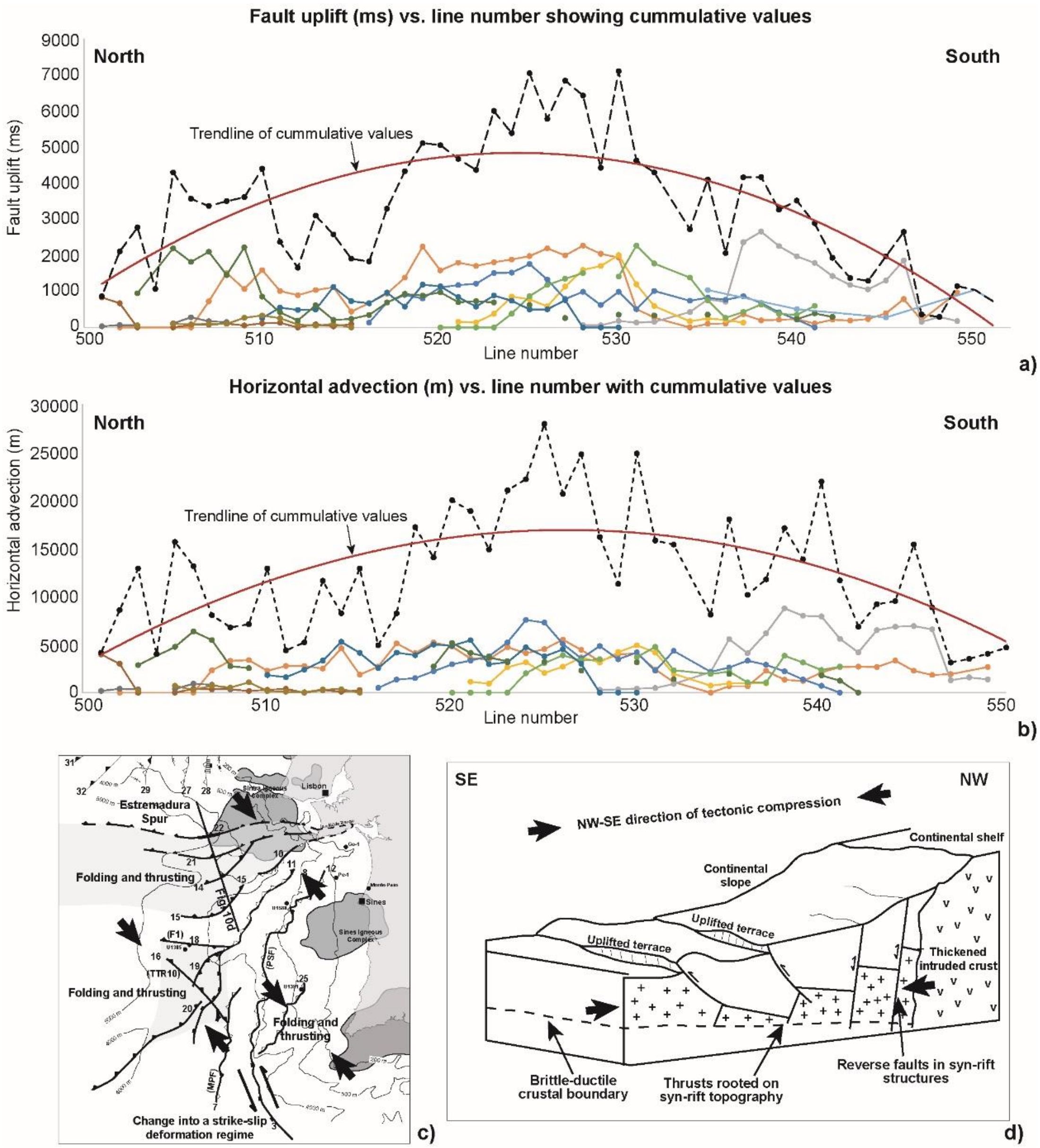

Figure 10: Cumulative data for fault uplift and horizontal advection as measured from north to south along SW Iberia. a) a typical C-shaped curved for uplift is observed when plotted against distance. b) a similar C-shaped curve is observed for horizontal advection, mimicking the results in the first graph (Fig. 10a). c) regional map summarising the tectonic setting observed in SW Iberia and justifying the generation of localised fold-and-thrust belts. D) 3D block diagram summarising the reactivation style of faults in the study area against a hard crustal buttress formed around the areas intruded by Late Cretaceous magma. 440

and just offshore this city, likely associated with the thickening of crust at its base, may justify the reason why the faults located to the west of SW Iberia indentor accumulated the bulk of uplift and horizontal advection in the study area. Finally, it may also explain why Alpine tectonics seems to be in its early stages of forming a subduction zone in SW Iberia, with this hard indentor concentrating strain under a prolonged, Late Cenozoic, setting dominated by NW-SE tectonic compression. In parallel, the presence of this indentor led to a cumulative tectonic uplift of >6 km in the mid-part of SW Iberia's Atlantic margin (Fig. 10).

8 Conclusions

Seismic and borehole data were used to quantify, for the first time, the true magnitude of tectonic uplift and inversion experienced by the Atlantic margin of SW Iberia. The recognition of geometric coherence in the faults mapped in SW Iberia hints at a degree of synchronous movement thus far not proven in the literature. The main conclusions of this study can be summarised as follows:

(1) The recognition of structural offset and oversteepened stratigraphic markers in SW Iberia demonstrates a magnitude of uplift of the Iberian Plate core that is, cumulatively, greater than previously assumed. Often assumed in the order of 1-1.5 km, the amount of Cenozoic tectonic uplift recorded by some of the faults mapped in SW Iberia exceeds 2 km and, cumulatively, can reflect a total uplift of > 6 km.

(2) Magmatic edifices and the intrusion of magma below the Late Cretaceous crust and basins led to the thermal uplift of large areas of SW Iberia. These areas were later reutilised as structural buttresses to Alpine compression, with the most developed inversion structures being developed around these buttresses.

(3) Geometric coherence in faults reveal these can be reactivated in tandem during the largest of seismic events, thus enhancing the seismogenic and tsunamigenic potential of SW Iberia. Faults reveal geometric coherence along the margin and, putatively, may be kinematically coherent when of the largest seismic events. Importantly, Fault 3 comprises a ~200 km long fault capable of generating Mw 8.0 earthquakes.

(4) The presence of a hard magmatic 'core' of rock in the mid part of SW Iberia, near Sines, justifies the formation of a structural indentor, and why the faults located to the west accumulated the bulk of uplift and horizontal advection. It also explains why Alpine tectonics is slowly progressing to forming a fully-developed subduction zone in the study area, with this hard indentor focusing tectonic deformation ahead of a thickened, hard intruded part of the West Iberian Margin. Similar uplifted, structural buttresses coincide with the Estremadura Spur in Central Portugal and the Sagres Plateau in Algarve.

Appendix A

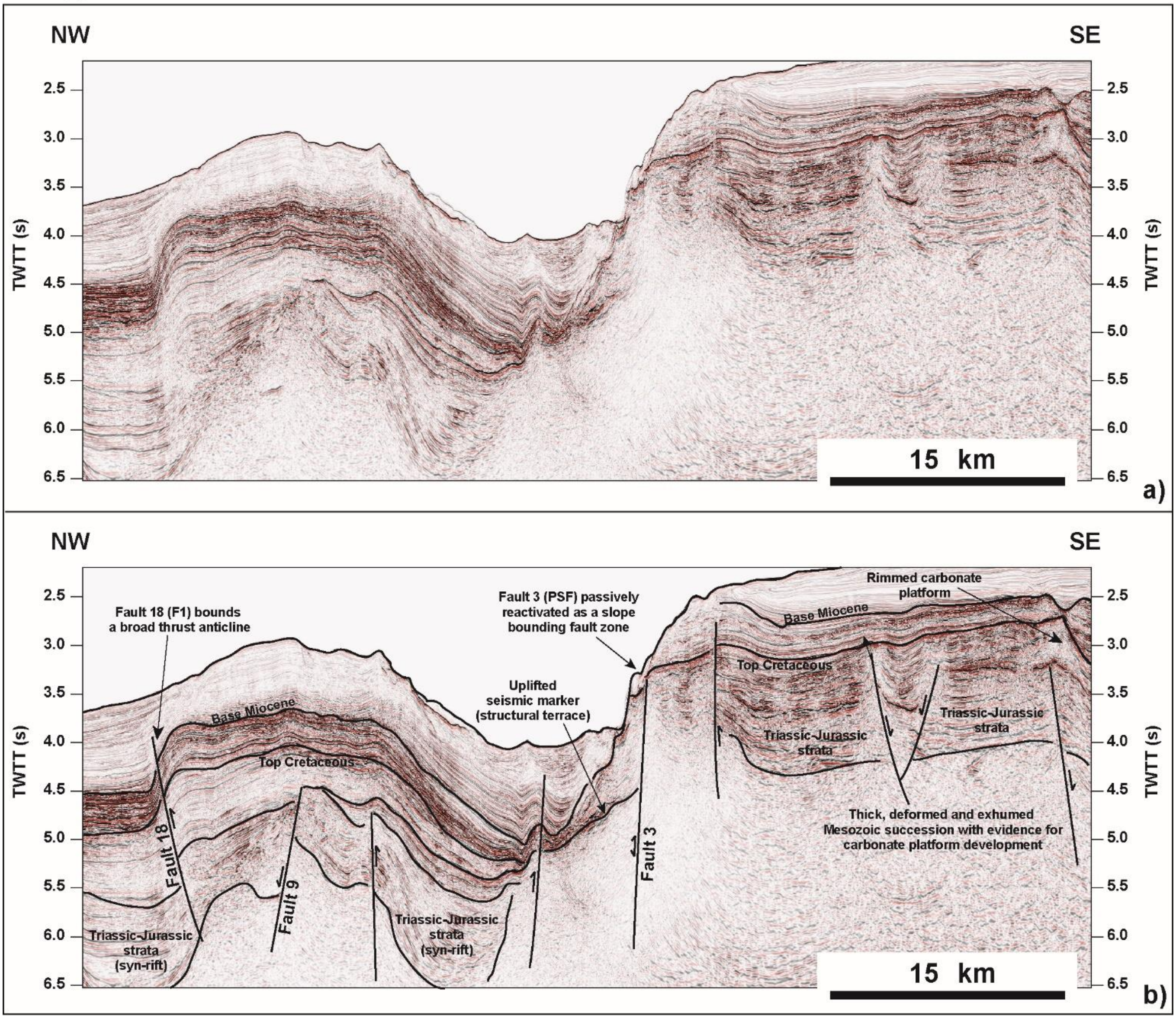

Figure A1: a) Uninterpreted and b) interpreted seismic profile from SW Iberia highlighting a vast area of Late Cretaceous erosion and exhumation to the east (i.e. landwards) from Fault 3. The region oceanwards from this same fault reveals a gentle thrust anticline and important evidence for shortening at upper crustal level. Note that Faults 3 and 18 are rooted in basement rocks and are likely related to the reactivation of a deep-crustal structures inherited from the syn-rift stage. The location of the seismic profile is shown in Fig. 1. Seismic data courtesy of TGS.

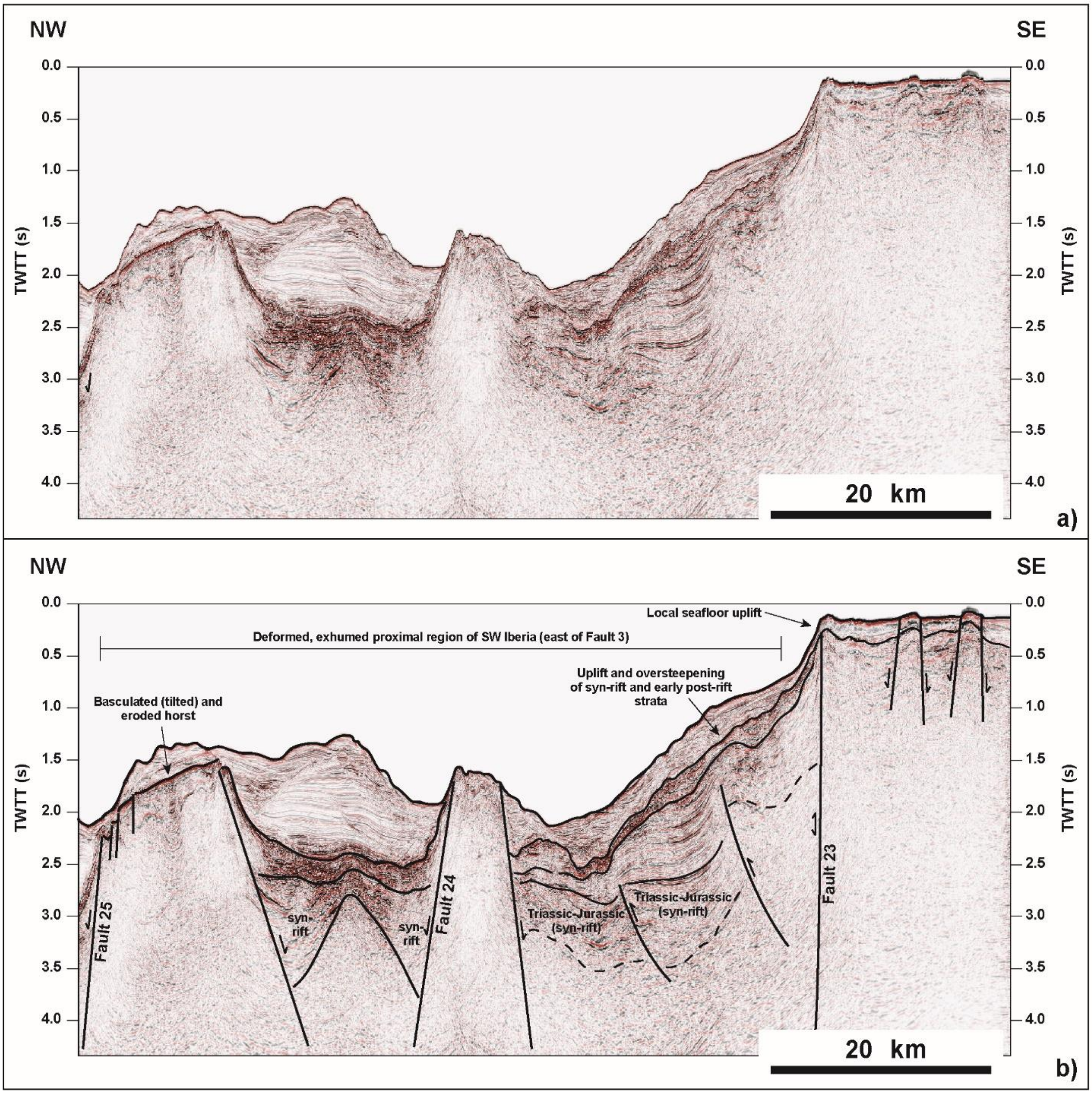

Figure A2: a) Uninterpreted and b) interpreted seismic profile from SW Iberia imaging the area next to Faults 23, 24 and 25, where important uplift is recorded in Mesozoic strata. These strata are oversteepened and uplifted near the most active faults in the study are, e.g. Fault 23. The location of the seismic profile is shown in Fig. 1. Seismic data courtesy of TGS.

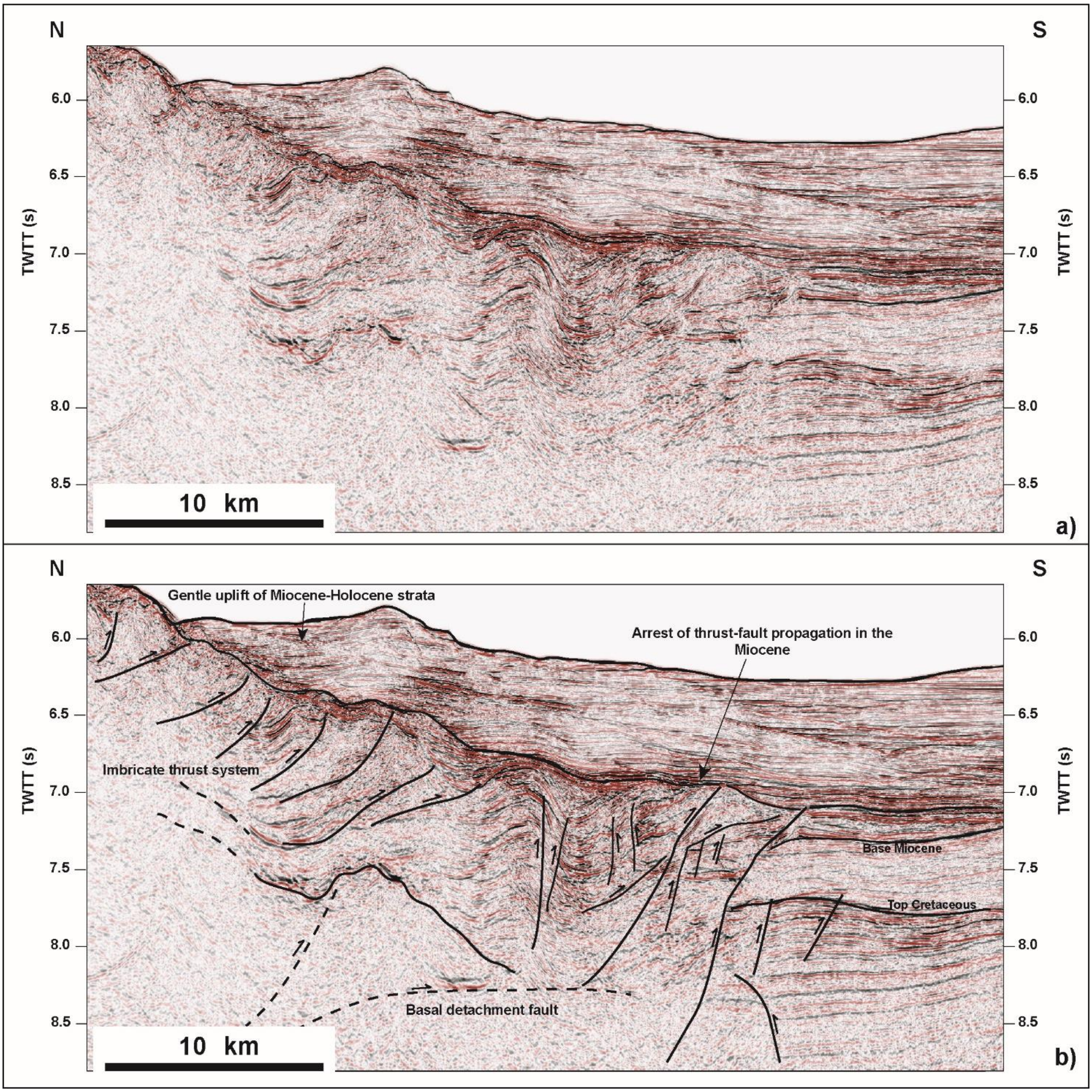

Figure A3: a) Uninterpreted and b) interpreted seismic imaging the southern flank of the Estremadura Spur and its youngest fold-and-thrust belt, Note the arrest of the folding and thrusting during the Miocene and, indirectly, the dating of the sediment apron west of Lisbon, on the continental rise, as being also Miocene to Holocene in age. The location of the seismic profile is shown in Fig. 1. Seismic data courtesy of TGS.

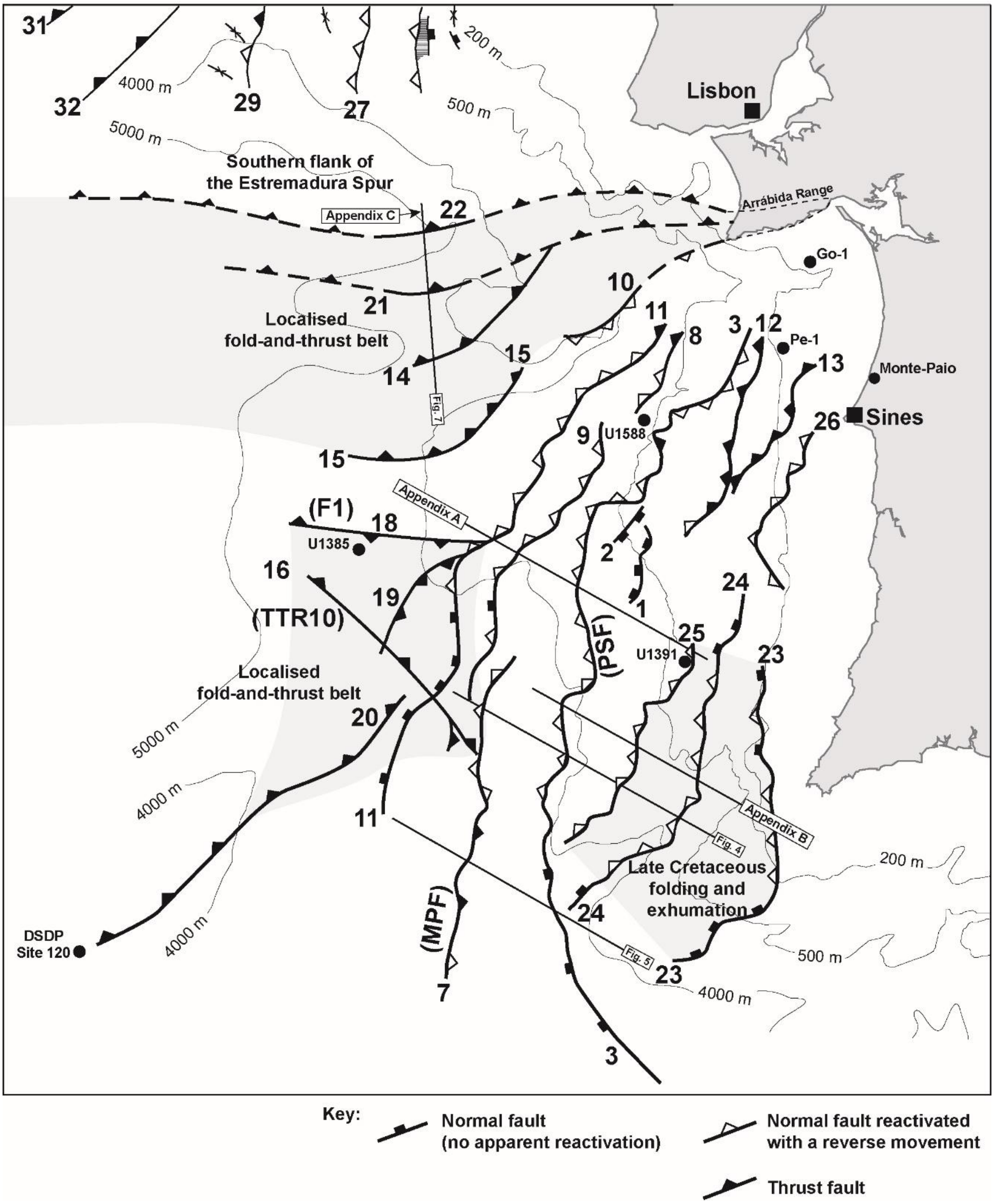

Figure A4: Structural map of SW Iberia highlighting main structures and their reactivation histories. Once again Structures mapped constitute long fault zones that are hard linked at depth to constitute >200 km long features as in the case of Fault 3.

Data and resources

The seismic data in this paper were provided by TGS and are available upon request. Getech provided the magnetic data in Figure 6, which are also available upon request. Bathymetric and seismological data for West Iberia, i.e. the locations and relative magnitudes of earthquakes for the period spanning 1900 to 2006, was obtained from GeoMapApp.

Author contribution

TMA wrote the manuscript, interpreted the seismic and borehole datasets, and designed all experiments in this paper.

Acknowledgements

The authors would like to acknowledge the reviewers for their constructive comments. Schlumberger for the support provided to the 3D Seismic Lab. TGS is acknowledged for the provision of seismic data on West Iberia. Data on Newfoundland was obtained from Natural Resources Canada.

References

Alves, T. M., Gawthorpe, R. L., Hunt, D. H., and Monteiro, J. H.: Cenozoic tectono-sedimentary evolution of the western Iberian margin, Mar. Geo., 195, 75-108, doi: 10.1016/S0025-3227(02)00683-7, 2003.

Alves, T. M., Moita, C., Cunha, T., Ullnaess, M., Myklebust, R., Monteiro, J. H., and Manuppella, G.: Diachronous evolution of Late Jurassic–Cretaceous continental rifting in the northeast Atlantic (west Iberian margin), Tectonics, 28, TC4003, doi: 10.1029/2008TC002337, 2009.

Bonilla, M. G., Mark, R. K., and Lienkaemper, J. J.: Statistical relations among earthquake magnitude, surface rupture length, and surface fault displacement, U.S. Geological Survey open-file report; 84-256, Gov. Doc. Number 19.76:84-256. https://pubs.usgs.gov/of/1984/of84-256/, 1984.

Capdevila R. and Mougenot D.: Pre-Mesozoic Basement of the Western Iberian Continental Margin and its Place in the Variscan Belt. In: Boillot G., Winterer E.J., et al. (Eds.), Proc. ODP, Sci. Results, 103, pp. 3-12, 1988.

Casson, M., Jeremiah, J., Calvès, G., de Goyet, F. V., Reuber, K., Bidgood, M., Rehákova, D., Bulot, L., and Redfern, J.: Evaluating the segmented post-rift stratigraphic architecture of the Guyanas continental margin, Petr. Geosc., 27, doi: 10.1144/petgeo2020-099, 2021.

Castañares, L. M. and Robles, S.: El vulcanismo del Albiense—Santoniense en la Cuenca Vasco-Cantábrica, In: Geología de España, Vera JA (ed.), Sociedad Geológica de España, Instituto Geológico y Minero de España, 306–308, 2004.

Comin-Chiaramonti, P., de Min, A., Girardi, V. A. V., and Ruberti, E.: Post-Paleozoic magmatism in Angola and Namibia: A review, In: Beccaluva, L., Bianchini, G., Wilson, M. (eds). Volcanism and Evolution of the African Lithosphere, GSA Sp. Papers 478, doi: 10.1130/2011.2478(12), 2021.

Cunha, P. P.: Cenozoic Basins of Western Iberia: Mondego, Lower Tejo and Alvalade Basins, In: Quesada, C. and Oliveira, J.T. (eds.). The Geology of Iberia: A Geodynamic Approach, Vol. 4, pp. 105-130, doi: 10.1007/978-3-030-11190-8_4, 2019.

Davis, K., Burbank, D. W., Fisher, D., Wallace, S., and Nobes, D.: Thrust-fault growth and segment linkage in the active Ostler fault zone, New Zealand, J. Str. Geol., 27, 1528-1546, doi:10.1016/j.jsg.2005.04.011, 2005.

Davison, I., Faull, T., Greenhalgh, J., Beirne, E. O., and Steel, I.: Transpressional structures and hydrocarbon potential along the Romanche Fracture Zone: a review, In: M. Nemčok, S. Rybár, S. T. Sinha, S. A. Hermeston, L. Ledvényiová (eds.), Transform Margins: Development, Controls and Petroleum Systems, Geol. Soc., London, Sp. Pub., 431, doi:10.1144/SP43, 2016.

Dinis, P. A., Vermeesch, P., Duarte, L., Cunha, P. P., Barbarano, M., and Garzanti, E.: The Variscan basement in the western shoulder of the Lusitanian Basin (West Iberian Margin): insights from detrital-zircon geochronology of Jurassic strata, J. Iberian Geol., 47, 685-696, doi: 10.1007/s41513-021-00177-w, 2021.

Duarte, J. C., Rosas, F. M., Terrinha, P., Schellart, W. P., Boutellier, D., Gutscher, M.-A., and Ribeiro, A.: Are subduction zones invading the Atlantic? Evidence from the southwest Iberia margin, Geology, 41, 839-842, doi:10.1130/G34100.1, 2013.

Elias, P. and Briole, P.: Ground Deformations in the Corinth Rift, Greece, Investigated Through the Means of SAR Multitemporal Interferometry, Geochem, Geophys,, Geosyst, 19, 4836-4857, doi: 10.1029/2018GC007574, 2018.

Fossen, H. and Rotevatn, A.: Fault linkage and relay structures in extensional settings—A review, Earth-Sci. Rev., 154, 14-28, doi: 10.1016/j.earscirev.2015.11.014, 2016.

Geldmacher, J., Hoernle, K., Klügel, A., Bogaard, P., Wombacher, F., and Berning, B.: Origin and geochemical evolution of the Madeira-Tore Rise (eastern North Atlantic), J. Geophys. Res., 111, B09206, doi: 10.1029/2005JB003931, 2016.

Giba, M., Walsh, J. J., and Nicol, A.: Segmentation and growth of an obliquely reactivated normal fault, J. Str. Geol., 39, 253-267, doi: 10.1016/j.jsg.2012.01.004, 2012.

Gràcia, E., Dañobeitia, J., Vergés, J., and the PARSIFAL Team: Mapping active faults offshore Portugal (36°N–38°N): Implications for seismic hazard assessment along the southwest Iberian margin, Geology, 31, 83-86, doi: 10.1130/0091-7613(2003)031<0083:MAFOPN>2.0.CO;2, 2003.

Grange, M., Scharer, U., Merle, R., Girardeu, J., and Cornen, G.: Plume–Lithosphere Interaction during Migration of Cretaceous Alkaline Magmatism in SW Portugal: Evidence from U–Pb Ages and Pb–Sr–Hf Isotopes, J. Petrol., 51, 1143-1170, doi: 10.1093/petrology/egq018, 2010.

Grevemeyer, I., Ranero, C. R., Papenberg, C., Sallares, V., Bartolomé, R., Prada, M., Batista, L., and Neres, M.: The continent-to-ocean transition in the Iberia Abyssal Plain, Geology 50, 615-619, doi: 10.1130/G49753.1, 2022.

Gutscher, M.-A., Dominguez, S., Westbrook, G. K., Le Roy, P., Rosas, F., Duarte, J. C., Terrinha, P., Miranda, J. M., Graindorge, D., Gailler, A., Sallares, V., and Bartolomé, R.: The Gibraltar subduction: A decade of new geophysical data, Tectonophys., 574-575, 72-91, doi: 10.1016/j.tecto.2012.08.038, 2012.

He, C., Yang, C.-J., Turowski, J. M., Rao, G., Roda-Boluda, D. C., and Yuan, X. P.: Constraining tectonic uplift and advection from the main drainage divide of a mountain belt, Nature Comm., 12, 544, doi: 10.1038/s41467-020-20748-2, 2021.

Hernández-Molina, F. J., Stow, D., Alvarez-Zarikian, C., and Expedition IODP 339 Scientists: IODP Expedition 339 in the Gulf of Cadiz and off West Iberia: decoding the environmental significance of the Mediterranean outflow water and its global influence, Sci. Drilling, 16, 1–11, doi: 10.5194/sd-16-1-2013, 2013.

Hodell, D. A., Abrantes, F., Alvarez Zarikian, C. A., and the Expedition 397 Scientists: Expedition 397 Preliminary Report: Iberian Margin Paleoclimate. International Ocean Discovery Program, doi: 10.14379/iodp.pr.397, 2023.

Jolivet, L., Baudin, T., Calassou, S., Chevrot, S., Ford, M., Issautier, B., Lasseur, E., Masini, E., Manatschal, G., Mouthereau, F., Thinon, I., and Vidal, O.: Geodynamic evolution of a wide plate boundary in the Western Mediterranean, near-field versus far-field interactions, Bull. . Soc. Géol. France, 192, 48, doi: 10.1051/bsgf/2021043, 2021.

Karabulut, H., Güvercin, S. E., Hollingsworth, J., and Konca, A. Ö.: Long silence on the East Anatolian Fault Zone (Southern Turkey) ends with devastating double earthquakes (6 February 2023) over a seismic gap: implications for the seismic potential in the Eastern Mediterranean region. J. Geol. Soc., London, 180, jgs2023-21, doi: 10.1144/jgs2023-021, 2023.

Kim, Y.-S. and Sanderson, D. J.: The relationship between displacement and length of faults: a review, Earth-Sci. Rev., 68, 317-334, doi: 10.1016/j.earscirev.2004.06.003, 2005.

Kimura, G., Koge, H., and Tsuji, T.: Punctuated growth of an accretionary prism and the onset of a seismogenic megathrust in the Nankai Trough, Prog. .Earth Plan. Sci., 5, 78, doi: 10.1186/s40645-018-0234-1, 2018.

Lei, C., Alves, T. M., Ren, J., and Tong, C.: Rift Structure and Sediment Infill of Hyperextended Continental Crust: Insights From 3D Seismic and Well Data (Xisha Trough, South China Sea), J. Geophys. Res.: Solid Earth, 125, e2019JB018610, doi: 10.1029/2019JB018610, 2020.

Maldonado, A., Somoza, L., and Pallarés, L.: The Betic orogen and the Iberian–African boundary in the Gulf of Cadiz: geological evolution (central North Atlantic), Mar. Geol., 155, 9-43, doi: 10.1016/S0025-3227(98)00139-X, 1999.

Mangano, G., Alves, T. M., Zecchin, M., Civile, D., and Critelli, S.: The Rossano–San Nicola Fault Zone evolution impacts the burial and maturation histories of the Crotone Basin, Calabrian Arc, Italy, Petr. Geosc., 29, petgeo2022-085, doi: 10.1144/petgeo2022-085, 2023.

Martín-Chivelet, J., Floquet, M., García-Senz, J., Callapez, P.M., López-Mir, B., Muñoz, J.A., Barroso-Barcenilla, F., Segura, M., Soares, A. F., Dinis, P. M., Marques, J. F., and Arbués, P.: Late Cretaceous Post-Rift to Convergence in Iberia, In: Quesada, C. and Oliveira, J.T. (eds.). The Geology of Iberia: A Geodynamic Approach, Vol. 3, pp. 285-376., doi: 10.1007/978-3-030-11295-0, 2019.

Martins, L. T., Madeira, J., Youbi, N., Munhá, J., Mata, J., and Kerrich, R.: Rift-related magmatism of the Central Atlantic magmatic province in Algarve, Southern Portugal, Lithos, 101, 102-124, doi: 10.1016/j.lithos.2007.07.010, 2008.

Mauffret, A., Mougenot, D., Miles, P. R., and Malod J.A.: Cenozoic deformation and Mesozoic abandoned spreading centre in the Tagus Abyssal Plain (west of Portugal): Results of a multichannel seismic survey, Can. J. . Earth Sci., 26, 1101– 1123, doi: 10.1139/e89-095, 1989.

Miranda, R., Valadares, V., Terrinha, P., Mata, J., Azevedo, M. R., Gaspar, M., Kullberg, J. C., and Ribeiro, C.: Age constraints on the Late Cretaceous alkaline magmatism on the West Iberian Margin, Cretaceous Res., 30, 575-586, doi: 10.1016/j.cretres.2008.11.002, 2009.

Monna, S., Argani, A., Cimini, G. B., Frugoni, F., and Montuori, C.: Constraints on the geodynamic evolution of the Africa–Iberia plate margin across the Gibraltar Strait from seismic tomography, Geosci. Frontiers, 6, 39-48, doi: 10.1016/j.gsf.2014.02.003, 2015.

Mougenot (1988). Geologie de la marge Portugaise, These de Doctorat D'Etat des Sciences Naturelles, Université Pierre et Marie Curie, Paris, 155 pp.

Neres, M. and Ranero. C. R.: An appraisal using magnetic data of the continent-to-ocean transition structure west of Iberia. Geophys. J. Int., 234, 1819-1934, doi: 10.1093/gji/ggad163, 2023.

Neves, M. C., Terrinha, P., Afilhado, A., Moulin, M., Matias, L., and Rosas, F.: Response of a multi-domain continental margin to compression: Study from seismic reflection–refraction and numerical modelling in the Tagus Abyssal Plain, Tectonophys., 468, 113-130, doi: 10.1016/j.tecto.2008.05.008, 2009.

Peacock. D. C. P.: Propagation, interaction and linkage in normal fault systems, Earth-Sci. Rev., 58, 121-142, doi: 10.1016/S0012-8252(01)00085-X, 2002.

Pereira, R. and Alves, T. M.: Crustal deformation and submarine canyon incision in a Meso-Cenozoic first-order transfer zone (SW Iberia, North Atlantic Ocean), Tectonophys., 601, 148-162, doi: 10.1016/j.tecto.2013.05.007, 2013.

Pereira, R., and Gamboa, D.: In situ carbon storage potential in a buried volcano, Geology, doi: 10.1130/G50965.1, 2023.

Pereira, R., Rosas, F., Mata, J., Represas, P., Escada, C., and Silva, B.: Interplay of tectonics and magmatism during post-rift inversion on the central West Iberian Margin (Estremadura Spur), Basin Res., 33, 1497-1519, doi: 10.1111/bre.12524, 2021.

Pereira, R., Mata, J., Ramalho, R. S., Rosas, F. M., Silva, B., Represas, P., and Escada, C.: Nature, timing and magnitude of buried Late Cretaceous magmatism on the central West Iberian Margin, Basin Res., 34, 771-796, doi: 10.1111/bre.12640, 2022.

Rodríguez-Salgado, P., Childs, C., Shannon, P. M., and Walsh, J. J.: Structural evolution and the partitioning of deformation during basin growth and inversion: A case study from the Mizen Basin Celtic Sea, offshore Ireland, Basin Res., 32, 830-853, doi: 10.1111/bre.12402, 2019.

Sachpazi, M., Clément, C., Laigle, M., Hirn, A., and Roussos, N.: Rift structure, evolution, and earthquakes in the Gulf of Corinth, from reflection seismic images, Earth Plan. Sci. Lett., 216, 243-257, doi: 10.1016/S0012-821X(03)00503-X, 2003.

Saspiturry, N., Issautier, B., Razin, P., Baudin, T., Asti, R., Lagabrielle, Y., Allanic, C., Serrano, O., and Duretz, T.: Review of Iberia–Eurasia plate-boundary basins: Role of sedimentary burial and salt tectonics during rifting and continental breakup, Basin Res., 33, 1626-1661, doi: 10.1111/bre.12529, 2020.

Schiffer, C., Doré, A. G., Foulger, G. R., Franke, D., Geoffroy, L., Gernigon, L., Holdsworth, B., Kusznir, N., Lundin, E., McCaffrey, K., Peace, A. L., Petersen, K. D., Phillips, T. B., Stephenson, R., Stoker, M. S., and Welford, J. K. Structural inheritance in the North Atlantic, Earth-Sci. Rev., 206, 102975, doi: 10.1016/j.earscirev.2019.102975, 2020.

Silva, P. G., Elez, J., Pérez-López, R., Giner-Robles, J. L., Gómez-Diego, P. V., Roquero, E., Rodríguez-Pascua, M. A., and Bardají, T. The AD 1755 Lisbon Earthquake-Tsunami: Seismic source modelling from the analysis of ESI-07 environmental data, Quat. Intern., 651, 6-24, doi: 10.1016/j.quaint.2021.11.006, 2023.

Somoza, L., Medialdea, T., Terrinha, P., Ramos, A., and Vazquez, J.-T.: Submarine active faults and morpho-tectonics around the Iberian Margins: Seismic and tsunamis hazards, Frontiers Earth Sci., 9, 2021, doi: 10.3389/feart.2021.653639, 2021.

Song, G., Wang, M., Jiang, D., Chen, Z., Yan, B., and Feng, W.: Along-strike structural linkage and interaction in an active thrust fault system: A case study from the western Sichuan foreland basin, China, Basin Res., 33, 210-226, doi: 10.1111/bre.12461, 2020.

Strganac, C., Salminen, J., Jacobs, L. L., Polcyn, M. J., Ferguson, K. M., Mateus, O., Shulp, A. S., Morais, M. L., Tavares, T. S., and Gonçalves, A. O.: Carbon isotope stratigraphy, magnetostratigraphy, and 40Ar/39Ar age of the Cretaceous South Atlantic coast, Namibe Basin, Angola, J. African Earth Sci., 99, 452-462, doi: 10.1016/j.jafrearsci.2014.03.003, 2014.

Sun, Q., Alves, T. M., Zhao, M., Sibuet, J., Calvès, G., and Xie, X.: Post-rift magmatism on the northern South China Sea margin, GSA Bull., 132, 2382-2396, doi:10.1130/B35471.1, 2020.

Sun, Q., Alves, T. M., Wu, S., Zhao, M., and Xie, X.: Early Miocene magmatism in the Baiyun Sag (South China Sea): A view to the origin of intense post-rift magmatism, Gondwana Res., doi: 10.1016/j.gr.2022.05.013, 2022.

Teboul, P-A., Kluska, J-M., Marty, N. C. M., Debure, M., Durlet, C., Virgone, A., and Gaucherm E. C.: Volcanic rock alterations of the Kwanza Basin, offshore Angola - Insights from an integrated petrological, geochemical and numerical approach, Mar. Petr. Geol., 80, 394-411, doi: 10.1016/j.marpetgeo.2016.12.020, 2017.

Terrinha, P., Pinheiro, L. M., Henriet, J.-P., Matias, L., Ivanov, M.K., Monteiro, J.H., Akhmetzhanov, A., Volkonskaya, A., Shaskin, P., and Rovere, M.: Tsunamigenic-seismogenic structures, neotectonics, sedimentary processes and slope instability on the southwest Portuguese Margin, Mar. Geol., 195, 55-73: doi: 10.1016/S0025-3227(02)00682-5, 2003.

Terrinha, P., Matias, L., Vicente, J., Duarte, J., Luís, J., Pinheiro, L., Lourenço, N., Diez, S., Rosas, F., Magalhães, V., Valadares, V., Zitellini, N., Roque, C., Mendez Vítor, L. and MATESPRO Team: Morphotectonics and strain partitioning at the Iberia–Africa plate boundary from multibeam and seismic reflection data, Mar. Geol., 267, 156-174, doi: 10.1016/j.margeo.2009.09.012, 2009.

Trippetta, F., Petricca, P., Billi, A., Collettini, C., Cuffaro, M., Lombardi, A. M., Scrocca, D., Ventura, G., Morgante, A., and Doglioni, C.: From mapped faults to fault-length earthquake magnitude (FLEM): a test on Italy with methodological implications, Solid Earth, 10, 1555-1579, doi: 10.5194/se-10-1555-2019, 2019.

Tsuji, T., Ashi, J., and Ikeda, Y.: Strike-slip motion of a mega-splay fault system in the Nankai oblique subduction zone, Earth, Plan. Space, 66, 120, doi: 10.1186/1880-5981-66-120, 2014.

Tucholke, B. E. and Sibuet, J.-C.: Leg 210 synthesis: tectonic, magmatic, and sedimentary evolution of the Newfoundland–Iberia rift. In: Tucholke, B.E., Sibuet, J.-C., Klaus, A. (Eds.), Proceedings of the ODP, Scientific Results, v. 210, Ocean Drilling Project, College Station, TX, pp. 1–56, 2007.

Ubide, T., Wijbrans, J. R., Galé, C., Arranz, E., Lago, M., and Larrea, P.: Age of the Cretaceous alkaline magmatism in northeast Iberia: Implications for the Alpine cycle in the Pyrenees, Tectonics, 22, 1444-1460, doi:10.1002/2013TC003511, 2014.

Vasconcelos, D. L., Bezerra, F. H. R., Clausen, O. R., Medeiros, W. E., de Castro, D. L., Vital, H., and Barbosa, J. A.: Influence of Precambrian shear zones on the formation of oceanic fracture zones along the continental margin of Brazil, Mar. Petr. Geol., 101, 322-333, doi: 10.1016/j.marpetgeo.2018.12.010, 2019.

Vissers, R. L. M., van Hinsbergen, D. J. J., van der Meer, D. G., and Spakman, W.: Cretaceous slab break-off in the Pyrenees: Iberian plate kinematics in paleomagnetic and mantle reference frames, Gondwana Res., 34, 49-59, doi: 10.1016/j.gr.2016.03.006, 2016.

Walsh, J. J. and Watterson, J.: Geometric and kinematic coherence and scale effects in normal fault systems, Geol, Soc., London, Sp. Pub., 56, 193-203, doi: 10.1144/GSL.SP.1991.056.01.13, 1991.

Walsh, J. J., Bailey, W. R., Childs, C., Nicol, A., Bonson, C. G.: Formation of segmented normal faults: a 3-D perspective, J. Str. Geol., 25, 1251-1262, doi: 10.1016/S0191-8141(02)00161-X, 2003.

Willemse, E. J. M., Peacock, D. C. P., Aydin, A.: Nucleation and growth of strike-slip faults in limestones from Somerset, U.K, J. Str. Geol., 19, 1461-1477, doi: 10.1016/S0191-8141(97)00056-4, 1997.

Willet, S. D. and Brandon, M.: On steady states in mountain belts, Geology, 30, 175-178, doi: 10.1130/0091-7613(2002)030<0175:OSSIMB>2.0.CO;2, 2002.

Willet, S. D., Slingerland, R., Hovius, N.: Uplift, shortening, and steady state topography in active mountain belts, Am. J. Sci., 301, 455-485, doi: 10.2475/ajs.301.4-5.455, 2001.

Wyss, M.: Estimating maximum expectable magnitude of earthquakes from fault dimensions, Geology, 7, 336-340, 1979.

Zhao, F., Alves, T. M., Wu, S., Li, W., Huuse, M., Mi, L., Sun, Q., Ma, B.: Prolonged post-rift magmatism on highly extended crust of divergent continental margins (Baiyun Sag, South China Sea), Earth Plan. Sci. Lett., 445, 79-91, doi: 10.1016/j.epsl.2016.04.001, 2016.

Zitellini, N., Gràcia, E., Matias, L., Terrinha, P., Abreu, M. A., DeAlteris, G., Henriet, J. P., Dañobeitia, J. J., Masson, D. G., Mulder, T., Ramella, R., Somoza, L., Diez, S.: The quest for the Africa–Eurasia plate boundary west of the Strait of Gibraltar, Earth Plan. Sci. Lett., 280, 13-50, doi: 10.1016/j.epsl.2008.12.005, 2009.